Studying the Halo Model with massive neutrinos

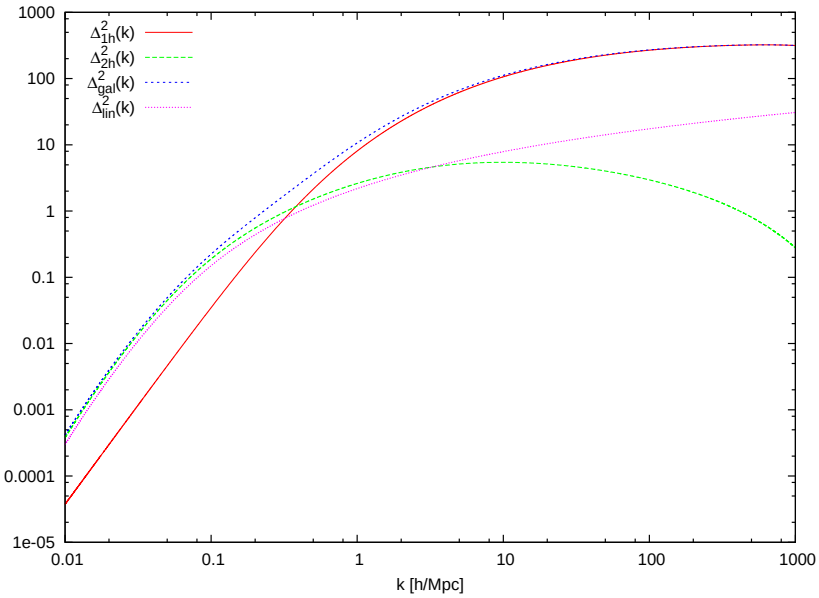

Master of Science thesis by

Kristin Charlotte Carlsson

Institute of Theoretical Astrophysics

University of Oslo

Norway

May 2008

Preface

At my school, there was a poster hanging in the physics lab. It showed a series of artistic renderings depicting the scales in the universe. It began with our place in the solar system, a rather large place in itself. Then, zooming outwards to reveal its place in the huge Milky Way galaxy, reducing the sun to an indistinguishable speck of dust in the process, it did not stop there: It continued outwards to dwarf this little sea of stars to show it was a part of the local group of galaxies with its vast, empty voids in between, before demonstrating what a rediculously small part that group of galaxies really is compared to what I learned was called superclusters. I like to believe that this poster was largely responsible for tipping the scales of my opinion that "astronomy is really fun and interesting" towards the direction "I am going to the university to study this stuff".

First of all I want to thank my supervisor prof. Øystein Elgarøy, for giving me a glimpse into the world of cosmological research, and also for his patience, for providing emergency rescue solutions when things got stuck, and for reminding me to take deep breaths every once in a while.

All the people whom I have come to know through my years at the university: DreamTeam members Silje, Espen and Michael most of all. Mahwash for being the first person I met at Blindern. Zoya, Anita and Nina for all the laughs. My colleagues at the study hall for making things social whenever I dangerously approached Hermit Stage.

I should also thank associate professor Frode K. Hansen, for providing in the cosmology course, among many other subjects, a qualitative and simple understanding of the power spectrum and its advantages. I stole a couple of sentences from his lectures in chapter two.

Much respect to the leaders in modern skepticism and defenders of science and good humor; James Randi, Richard Dawkins, Phil Plait, PZ Myers, Carl Sagan, Douglas Adams. For giving me the yearning to continue to learn about what I have come to realize is the most awe-inspiring and mysterious thing out there: Reality.

Sources of procrastination: Neil Gaiman. Lolcats. iTunes. Battlestar Galactica. The Blogosphere. In this case, I am not sure whether I wish to give *thanks* as such (honorable mentions at the most).

Personally I think I want to thank Michael Katz most of all, for simply being there all the time; for inspiring me through his hard work on his own master thesis, and at the same time congratulate him for winning first prize in his admirable single-handed, everyday tackling of what could only be described as another person's otherworldly moodswings and inconceivable fits of frustration, while at the same time bothering to make dinner. Thank you.

Kristin C. Carlsson
Oslo, May 16, 2008

Contents

List of Figures

List of Tables

Chapter 1

Introduction

> It's only been in the past few decades that the very biggest thing of all—the Universe—has been tied to the smallest things of all—subatomic particles. The very small and the very big are connected in a fundamental way, and it's only been through science that we've percieved that connection.
>
> —Phil Plait, "The Bad Astronomer"

1.1 The unseen universe

Physical cosmology encompasses a vast number of subjects. Even so, one may say that at least one of three factors always comes into play: The cosmologist either has to handle the very large, the very distant or the very long ago. Most of the time it will be a linear combination of the three, and in this sense cosmology plays the part as the "biggest" of natural sciences.

The universe is a place where most of the matter in it is invisible to our own curious eyes and telescopes. This somewhat mysterious *dark matter* is only perceived through its gravitational influence on large mass structures, such as the observed counterintuitive rotation of galaxies: When plotting the orbital velocity of the gas or stars in a galaxy against its distance from the galaxy center, one finds that these velocities are constant over a large range of distances, when it is expected that they should follow the dynamics of a Newtonian potential, much like the planets in our solar system. This discrepancy is thereby proposed to be filled by the presence of a type of matter which does not emit observable radiation, but acts through gravity to give a different rotation profile than would, at first glance, be anticipated.

To this day, the answer to what type of particles constitute dark matter has not been found, although the progress of natural science has steadily continued to rule out a number of proposals. Moreover, even matter itself, be it visible or dark, does not even take up more than a third of the energy available in the cosmos: By today's best standards in research a perhaps even more enigmatic factor, dubbed the cosmological constant[1], may have come

[1] A rather successful resurrection of "Einstein's greatest blunder"

to dominate the energy density of our universe, making it expand at the accelerating rate one can observe today.

It is interesting to note, then, that while the universe truly is the largest object to study, the most fundamental connection of all is still towards the very smallest constituents of particle physics.

Dark matter is not only needed to explain the rotation curves of galaxies, but to explain the structure of the universe altogether. This inevitably brings us to the topic of structure formation. The formation of mass structure through gravitational instability, i.e. that initially small fluctuations in density are amplified by gravity, can safely be regarded as the standard paradigm by which modern cosmologists prefer to model our universe. One possible explanation for the origin of these fluctuations is that they are quantum fluctuations puffed up to macroscopic scales during a period of inflation.

Furthermore, observations of how the matter is distributed on different length scales in the universe are an important test of cosmological models. For example, such observations can give an upper limit of the masses of neutrinos: As the portion of the dark matter consisting of neutrinos increases, less structure on the smaller scales may be observed. One of the most frequently used methods for measuring the matter distribution in the universe is to measure the statistical distribution of galaxies in the local universe. These *redshift surveys* have currently measured the position and redshift of hundreds of thousands of galaxies, with many more to come in the future.

One potential problem with this method is that it is based on the matter we can see, while what we really are interested in is the distribution of both dark and luminous matter combined. If dark and luminous matter have the same statistical distribution, then there are no problems with using measurements on observed galaxies only. Still, it seems that the two components in question are unevenly distributed on different length scales. The relationship between the distributions of the dark and luminous matter is called the bias factor, and it is difficult to calculate theoretically. There is, however, a simple model—the so-called *halo model*—where this type of bias can be taken into account.

1.2 Outline of the thesis

1.2.1 Problem

This thesis will give an introduction to the halo model and the concepts behind it. There are many ways and many degrees of detail with which to construct it, and the approach used here will be largely based on analytical approximations and empirical results.

With this model, an attempt will then be made to investigate the effects of massive neutrinos: In this picture, one may add neutrinos as a part of dark matter and study the effect on the statistical distribution of galaxies. The main points of interest are

- What are the effects on the clustering of galaxies on small scales by including massive neutrinos?

- Are these effects interesting, i.e. can the model be used to predict reasonable upper limits for the neutrino mass?

1.2.2 Layout

This chapter serves as a qualitative introduction to the field of cosmology and dark matter, as well as the questions within—a couple of which this thesis will try to answer. Chapter 2 attempts to give a theoretical motivation for the physical tools used in the study of large-scale structure and the part the neutrino plays in the picture. Chapter 3 introduces some key ingredients of the halo model itself. The numerical methods and implementations used for calculating the relevant parameters in the halo model is described in Chapter 4. Results are laid out in Chapter 5, while Chapter 6 summarizes and makes some concluding remarks.

Chapter 2

Theoretical background

In order to obtain a fundamental understanding of the halo model, it will be necessary to undergo a crash course in simple gravitational structure formation. Bound objects in the universe, such as galaxies and clusters of galaxies, are highly nonlinear structures, and are therefore generally much more difficult to study theoretically than linear density perturbations. There is, however, a simple model which might catch some important features of the formation of bound structures: The so-called spherical collapse model. This model will be considered in the first section.

In cosmology, one is also interested in the statistical distribution of so-called virialized structures, which will be explained below, and to answer questions such as "How many structures with mass less than a given value are we expected to find within a given, arbitrary volume?" The mass function is an important quantity that tells us something about how gravitationally bound structures of different mass is distributed in the universe. Later in this chapter will be considered a simple analytical model for the formation of structure, and an attempt is made to find the mass function in this model.

Further on in the chapter, the concept of the two-point correlation function and the closely related power spectrum is introduced; these are crucial elements in the study of and research in the large-scale structure of the universe.

The final theoretical ingredient is that of the neutrino, which will be given a short fact-sheet presentation in the last section of this chapter.

Much of the theoretical descriptions in this chapter are taken from various introductionary texts in cosmology, such as [1, 2, 3, 4, 5] and [6]. Refer to these for further reading on the concept of basic cosmology.

2.1 Virializing a sub-universe: Spherical collapse

We start out with a flat, matter dominated universe, called an Einstein-de Sitter (EdS) universe, placing within it a spherical region with density higher than the critical value $\rho_{\rm cr} \equiv 3H_0/8\pi G$. Here H_0 is the value of the Hubble parameter today (denoted by the subscript 0), and G is the gravitational constant. In cosmology, H_0 is often expressed

through $H_0 = 100h$ km s^{-1} Mpc^{-1}, so that h is dimensionless.

It is possible to show that this overdense spherical region can be treated as a separate sub-universe. In short, this is explained by the fact that the Poisson equation, which tells us about the relation between the density of matter and the gravitational potential, is linear, and therefore the effects of the homogeneous matter distribution and that of density fluctuations can be considered separately. The gravitational field of the total matter distribution is then the sum of the average matter distribution and that of the fluctuations. Since the density of this sub-universe is above $\rho_{\rm cr}$, it will behave like a closed model. In terms of the density parameter $\Omega_{\rm m0} \equiv \rho_{\rm m0}/\rho_{\rm cr}$ for matter, where the matter density is $\rho_{\rm m} = \rho_{\rm m0}a^{-3}$, such a universe is described by the Friedmann equation

$$\frac{H^2(t)}{H_0^2} = \frac{\Omega_{\rm m0}}{a^3} + \frac{1-\Omega_{\rm m0}}{a^2}. \tag{2.1}$$

Here $H(t) = \dot{a}/a$, where the dot implies differentiation with respect to cosmic time t, and $a = a(t)$ is the scale factor of the universe model in question. The curvature term scales as a^{-2}. From (2.1), and the criterium that $\dot{a} = 0$ for some finite value of a after a time of expansion, we find an expression for the maximal value the scale factor can achieve:[1]

$$\frac{\Omega_{\rm m0}}{a_{\rm max}^3} = \frac{\Omega_{\rm m0}-1}{a_{\rm max}^2} \quad \Leftrightarrow \quad a_{\rm max} = \frac{\Omega_{\rm m0}}{\Omega_{\rm m0}-1}. \tag{2.2}$$

At this value, the sub-universe has reached a turnaround and will start to contract. Equation (2.1) can be written as

$$\begin{aligned}
\left(\frac{{\rm d}a}{{\rm d}t}\right)^2 \frac{1}{H_0^2 a^2} &= \frac{\Omega_{\rm m0}}{a^3} + \frac{1-\Omega_{\rm m0}}{a^2} \\
\Rightarrow H_0 {\rm d}t &= \frac{{\rm d}a}{\sqrt{\frac{\Omega_{\rm m0}}{a} + 1 - \Omega_{\rm m0}}} \\
&= \frac{1}{\sqrt{\Omega_{\rm m0}-1}} \frac{\sqrt{a}{\rm d}a}{\sqrt{a_{\rm max}-a}}.
\end{aligned} \tag{2.3}$$

where we also have incorporated (2.2). Integrating this by demanding $t = 0$ when $a = 0$, we get

$$H_0 t = \frac{1}{\Omega_{\rm m0}-1} \int_0^a \frac{\sqrt{a'}{\rm d}a'}{\sqrt{a_{\rm max}-a'}}. \tag{2.4}$$

The following substitution can then be used:

$$a = a_{\rm max} \sin^2\left(\frac{\theta}{2}\right) = \frac{a_{\rm max}}{2}(1-\cos\theta), \tag{2.5}$$

[1] We also see that this criterium demands that $\Omega_{\rm m0} > 1$.

One can easily transform Eq. (2.4) to yield

$$\begin{aligned} H_0 t &= \frac{1}{2}\frac{\Omega_{\rm m0}}{(\Omega_{\rm m0}-1)^{3/2}}\int_0^\theta (1-\cos\theta')\mathrm{d}\theta' \\ &= \frac{\Omega_{\rm m0}}{2(\Omega_{\rm m0}-1)^{3/2}}(\theta-\sin\theta). \end{aligned} \tag{2.6}$$

The solution of (2.1) can therefore be written parameterized as

$$a(t) = A(1-\cos\theta) \tag{2.7}$$

$$t = B(\theta-\sin\theta) \tag{2.8}$$

where $A = a_{\rm max}/2$ and $B = \Omega_{\rm m0}/[2H_0(\Omega_{\rm m0}-1)^{3/2}]$. At its maximal size $a_{\rm max}$, we see that Eq. (2.7) gives an expression for the maximal value of θ:

$$a_{\rm max} = \frac{a_{\rm max}}{2}(1-\cos\theta_{\rm max}), \tag{2.9}$$

in turn giving $\cos\theta_{\rm max} = -1$ and thus $\theta_{\rm max} = \pi$. Using this on (2.8) is found

$$\begin{aligned} t_{\rm max} &= \pi B \\ &= \frac{\pi}{2H_0}\frac{\Omega_{\rm m0}}{(\Omega_{\rm m0}-1)^{3/2}}, \end{aligned} \tag{2.10}$$

which will be used in the following.

The mass density of the background universe behaves normally, which means it is given by $\rho_{\rm EdS} \propto a_{\rm EdS}^{-3}$, where $a_{\rm EdS}(t) = (t/t_0)^{2/3}$ describes the scale factor of the EdS model, with $t_0 = 2/3H_0$. This can be used to calculate the ratio between the overdensity of the spherical inhomogeneity and that of the EdS universe. At $a_{\rm max}$, we have

$$\begin{aligned} \frac{\rho_{\rm max}}{\rho_{\rm EdS,max}} &= \frac{\rho_{m0}a_{\rm max}^{-3}}{\rho_{\rm cr}a_{\rm EdS}^{-3}(t_{\rm max})} = \Omega_{\rm m0}\left(\frac{a_{\rm EdS}(t_{\rm max})}{a_{\rm max}}\right)^3 \\ &= \frac{t_{\rm max}^2(\Omega_{\rm m0}-1)^3}{t_0^2\Omega_{\rm m0}^2} \\ &= \frac{\frac{\pi^2}{4H_0^2}\frac{\Omega_{\rm m0}^2}{(\Omega_{\rm m0}-1)^3}(\Omega_{\rm m0}-1)^3}{\frac{4}{9H_0^2}\Omega_{\rm m0}^2} \\ &= \frac{9\pi^2}{16} \approx 5.55, \end{aligned} \tag{2.11}$$

having used expressions (2.2) and (2.10). This means that as the sphere had reached its maximum size, it was still more than five times denser than the background.

Since the spherical overdensity has no inner pressure in this simplified model, it will, after having reached its maximum size, collapse to zero radius and infinite density. Looking

at the symmetry in (2.7)–(2.8), this happens at $\theta = 2\pi$, i.e. when $t = 2\pi B$. As we can see from equation (2.10), this also equals $2t_{\max}$. In practice, various physical processes will interfere and stop the perturbation from collapsing to infinite density. For example, pressure gradients will grow sufficiently that the collapse stops. After all, the statement that $p = 0$ for non-relativistic matter is only an approximation; sooner or later during the collapse this approximation will no longer apply, and we must take pressure into consideration. If the perturbation does not end up a black hole, the result will be a system which satisfies the virial theorem (the system is *virialized*). The virial theorem provides a simple relation between between the expectation values of the kinetic energy K and the potential energy V of a system,

$$\langle K \rangle = \frac{1}{2}\langle V \rangle. \tag{2.12}$$

For a sphere of total mass M and radius a, one can show that the potential energy is

$$V = -\frac{3}{5}\frac{GM^2}{a}. \tag{2.13}$$

When the spherical perturbation reaches its maximum radius $a_{\max}$, the kinetic energy is zero, so that the total energy equals the potential energy,

$$E_{\text{tot}} = V_{\max} = -\frac{3}{5}\frac{GM^2}{a_{\max}}. \tag{2.14}$$

After this, the radius of the sphere decreases, until the system is virialized, where we have the situation

$$E_{\text{tot}} = K_{\text{vir}} - \frac{3}{5}\frac{GM^2}{a_{\text{vir}}}. \tag{2.15}$$

What we demand here is of course that the total energy is conserved in the two cases, so that the right-hand sides of equations (2.14) and (2.15) can be compared:

$$-\frac{3}{5}\frac{GM^2}{a_{\max}} = K_{\text{vir}} - \frac{3}{5}\frac{GM^2}{a_{\text{vir}}}. \tag{2.16}$$

Using (2.12), we see that the virial theorem is fulfilled when

$$K_{\text{vir}} = \frac{3}{10}\frac{GM^2}{a_{\text{vir}}}. \tag{2.17}$$

Substituting this and solving for a_{vir} finally gives

$$a_{\text{vir}} = \frac{a_{\max}}{2}. \tag{2.18}$$

The total mass density of the sphere at maximal radius is

$$\rho_{\max} = \rho(a_{\max}) = \frac{3M}{4\pi a_{\max}^3}, \tag{2.19}$$

while after virialization it is

$$\rho_{\rm vir} = \rho(a_{\rm max}/2) = \frac{24M}{4\pi a_{\rm max}^3}, \tag{2.20}$$

that is, eight times more dense than at the maximum radius.

Let us return to equation (2.7) and find out at which value $\theta = \theta_{\rm vir}$ the virial theorem is fulfilled. Dividing by a factor of $a_{\rm max}$ on both sides, we end up with

$$1 = \cos\theta_{\rm vir} - 1 \Rightarrow \cos\theta_{\rm vir} = 0. \tag{2.21}$$

This is fulfilled when $\theta_{\rm vir} = \{\pi/2, 3\pi/2\}$, but since we are interested in the period during collapse, i.e. when $\theta > \pi$, we get the answer $\theta_{\rm vir} = 3\pi/2$. We can then insert this into (2.8) and get an expression for at which time this happens:

$$\begin{aligned} \frac{t_{\rm vir}}{t_{\rm max}} &= \frac{\frac{3\pi}{2} - \sin\frac{3\pi}{2}}{\pi - \sin\pi} \\ &= \frac{\frac{3\pi}{2} + 1}{\pi} \\ &= \frac{3}{2} + \frac{1}{\pi} \approx 1.82. \end{aligned} \tag{2.22}$$

Remembering that the density of the background universe goes like $(t/t_0)^{-2}$, we can calculate the factor by which this density has decreased during the time period from $t_{\rm max}$ to $t_{\rm vir}$:

$$\begin{aligned} \frac{\rho_{\rm EdS,vir}}{\rho_{\rm EdS,max}} = \frac{\rho_{\rm EdS}(t_{\rm vir})}{\rho_{\rm EdS}(t_{\rm max})} &= \frac{(t_0/t_{\rm vir})^2}{(t_0/t_{\rm max})^2} \\ &= \left(\frac{t_{\rm max}}{t_{\rm vir}}\right)^2 \\ &\approx \left(\frac{1}{1.82}\right)^2 \approx \frac{1}{3.31}. \end{aligned} \tag{2.23}$$

Lastly, let us calculate the density contrast of the spherical perturbation in terms of the background universe, at the period of virialization. It is defined as

$$\delta_{\rm vir} = \frac{\rho_{\rm vir} - \rho_{\rm EdS,vir}}{\rho_{\rm EdS,vir}} = \frac{\rho_{\rm vir}}{\rho_{\rm EdS,vir}} - 1. \tag{2.24}$$

Relating the fraction in (2.24) to the expressions we have found so far, we find, via equations (2.11), (2.20) and (2.23), the overdensity to be

$$\begin{aligned} \delta_{\rm vir} &= \frac{\rho_{\rm vir}}{\rho_{\rm EdS,vir}} - 1 \\ &= \frac{\rho_{\rm vir}}{\rho_{\rm max}} \frac{\rho_{\rm max}}{\rho_{\rm EdS,max}} \frac{\rho_{\rm EdS,max}}{\rho_{\rm EdS,vir}} - 1 \\ &\approx 8 \times 5.55 \times 3.31 \approx 150. \end{aligned}$$

In reality, one could expect the process of virialization to take a little longer than predicted by our symmetrically simplified model, and it is indeed common to assume that that $a_{\rm vir}$ is in fact only reached after the time roughly corresponding to collapse. The process causing this is the lack of perfectly radial orbits of the particles in our sphere: Because of small-scale density and gravitational fluctuations occuring within the spherical region, increasing with density, there will be deviations of the particle orbits and scattering on the fluctuations—a process called *violent relaxation*. One would then get a value $1 + \delta_{\rm vir} = 18\pi^2 \approx 178$ for the density contrast, as shown in e.g. [7].

The overdensity at virialization is an important parameter in the model considered for this thesis, and in the following chapters, for conventional reasons, it will be denoted by the symbol $\Delta_{\rm vir}$. The sub-universe therefore has a density $\Delta_{\rm vir}$ times the background density $\bar{\rho}$.

To introduce an important parameter in the theory of spherically virialized objects, we return to the parametric solution of the Friedmann equation, Eqs. (2.7) and (2.8). Looking at the linear regime by expanding the expressions to the second order in θ (see Eqs. (A.4) and (A.5) in Appendix A for the sine and cosine expressions), one finds

$$\frac{a(t)}{a_{\rm max}} \approx \frac{\theta^2}{4} - \frac{\theta^4}{48}, \tag{2.25}$$

$$\frac{t}{t_{\rm max}} \approx \frac{1}{\pi}\left(\frac{\theta^3}{6} - \frac{\theta^5}{120}\right) \tag{2.26}$$

remembering that $t_{\rm max} = \pi B$. These expressions can be combined via iteration to yield the so-called linearized scale factor:

$$\frac{a^{\rm lin}(t)}{a_{\rm max}} \approx \frac{1}{4}\left(6\pi\frac{t}{t_{\rm max}}\right)^{2/3}\left[1 - \frac{1}{20}\left(6\pi\frac{t}{t_{\rm max}}\right)^{2/3}\right]. \tag{2.27}$$

This expression gives the linear theory prediction for the growth of a spherical perturbation. The lowest order truncation of (2.27), i.e. removing the square-bracketed part, is the expansion of the flat background universe. Because matter domination is assumed, and density therefore scales as a^{-3}, the linear prediction density contrast therefore is expressed as

$$1 + \delta^{\rm lin} = \left(\frac{a^{\rm lin}_{\rm EdS}}{a^{\rm lin}(t)}\right)^3, \tag{2.28}$$

which through substitution and further linearization will give

$$\delta^{\rm lin} = \frac{3}{20}\left(\frac{t}{t_{\rm max}}\right)^{2/3}. \tag{2.29}$$

Inserting $t_{\rm max} = \pi B$ and $t = t_{\rm vir} = 2t_{\rm max}$ gives the linearly predicted value of the density contrast, corresponding to the epoch of gravitational spherical collapse:

$$\delta_c = \frac{3}{20}(12\pi)^{2/3} = 1.686. \tag{2.30}$$

Before understanding the important role this linear value plays in nonlinear analytical theory, the next section will look at a vital tool in precision cosmology when determining the distribution of structure on large scales.

2.2 Intermezzo: The power spectrum

To classify structure with regards to the matter perturbations in the universe, a simple yet powerful statistic is the *two-point correlation function*. Generally, we write the n-point correlation function of density fluctuations $\delta(\mathbf{x}_i)$ as

$$\xi_n(\mathbf{x}_1, \ldots, \mathbf{x}_n) \equiv \langle \delta(\mathbf{x}_1) \cdots \delta(\mathbf{x}_n) \rangle_c, \tag{2.31}$$

where the angular brackets denote an average over the probability distribution of the perturbations. If all $\mathbf{x}$ are the same, we can write

$$\xi_n = \langle \delta^n \rangle_c. \tag{2.32}$$

The one-point correlation function in this case is simply the expectation value, $\langle \delta \rangle_c = \langle \delta \rangle$, and the two-point (auto-)correlation function (often referred to as simply the two point function) is defined as the variance,

$$\xi_2 = \langle \delta^2 \rangle_c = \langle \delta^2 \rangle - \langle \delta \rangle^2 \equiv \sigma^2. \tag{2.33}$$

In the case of galaxies, for example, one can define the two-point function

$$\langle \delta(\mathbf{x}_1)\delta(\mathbf{x}_2) \rangle = \xi_2(|\mathbf{x}_1 - \mathbf{x}_2|) = \xi_2(\mathbf{r}) = \xi_2(r) \tag{2.34}$$

as a measure of the probability of finding another galaxy at a radius r from one galaxy which is randomly placed in a given location—a definition from Peebles (1980) [8]. It can furthermore be thought of as a measure of clumpiness: The higher the value for some distance scale, the more matter is grouped together at that distance scale. However, the latter way of interpreting becomes a lot more clear if we transform the function into Fourier space. The Fourier transform of the two-point correlation function is called the *power spectrum*, and it is defined through

$$\langle \delta(\mathbf{k})\delta(\mathbf{k}') \rangle = (2\pi)^3 \delta_D(\mathbf{k} - \mathbf{k}') P(k). \tag{2.35}$$

Here δ_D is the Dirac delta function (not to be confused with the perturbation δ), which constrains $\mathbf{k}' = \mathbf{k}$, and the isotropy of the behaviour of fluctuations, as in x-space, gives $P(\mathbf{k}) = P(k)$. The scale k is the inverse of what we may call the wavelength of the Fourier space perturbation, defined in the usual way as a wavenumber, $k = 2\pi/\lambda$.

2.2.1 The shape of the power spectrum

One possible explanation for the origin of density fluctuations in the universe is that they are quantum fluctuations, amplified from subnuclear to astronomical scales during an extremely short period of inflation (lasting about 10^{-34} seconds) in the earliest stages of the universe. The amplitude of fluctuations on different length scales immediately after inflation is described by the primordial power spectrum, usually assumed to behave like a power law; $P(k) \propto k^n$. A popular choice is the scale-invariant power spectrum, in which the spectral index $n = 1$. This is a form independently proposed by Harrison and Zel'dovich in 1970, and current observations do indeed indicate a spectral index which is close to unity.

The power spectrum evolves, however, from this simple power law. A number of processes lead to the fact that perturbation growth depends on the matter content. For example, when the universe was radiation dominated, pressure effectively worked against gravity on wavelengths smaller than the size of the particle horizon at that epoch. Free-streaming is another important factor. Certain dark matter particles will, at early times, stream freely out of overdense regions into neighboring underdense ones, due to the particles being relativistic at that time. This leads to the smudging-out of structure on certain scales, and the random velocities of the dark matter particles determines the scales up to which density fluctuations are erased. Hot dark matter (HDM) particles (a suitable candidate of which will be discussed closer throughout this thesis, beginning in the next section) remain ultrarelativistic through the era of matter-radiation equality, $a_{\rm eq}$, and their free-streaming erases fluctuations up to the scale of super-clusters. Cold dark matter (CDM) particles become non-relativistic at much earlier times (hence the label "cold"), and preserves fluctuations on practically all scales. The effect on the power spectrum of such processes are summed up in the *transfer function*, the ratio of the amplitude of a density fluctuation on a certain scale today, and its amplitude when it entered the horizon.[2] Without further details, the power spectrum today can be written as the primordial form times the square of the transfer function:

$$P(k) \propto k^n T^2(k). \tag{2.36}$$

The overall effect of the transfer function is that the power spectrum turns over from the primordial shape at a scale which corresponds to the horizon scale at matter-radiation equality, as shown in Figure 2.1. The transfer function depends on cosmology, and different numerical fits have been inferred in order to model it.

The power spectrum has dimensions of k^{-3}, and it is useful to introduce the dimensionless power spectrum by

$$\Delta^2(k) \equiv \frac{k^3 P(k)}{2\pi^2}. \tag{2.37}$$

[2]Rather than describing the perturbation as entering the horizon, a more intuitive way of saying it would be the horizon becoming large enough to enclose the perturbation.

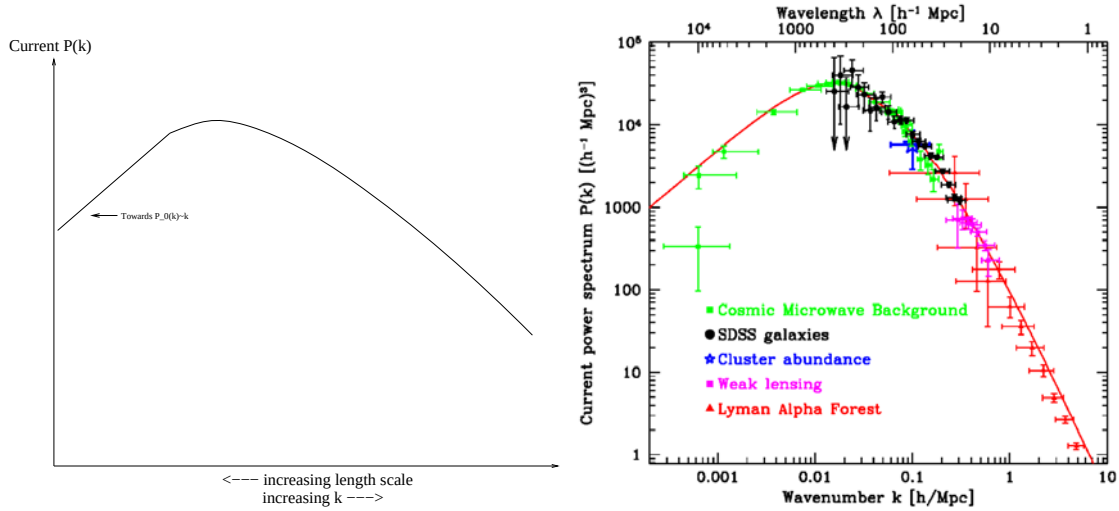

(a) (b)

Figure 2.1: The matter power spectrum today. (a) is a rough sketch which demonstrates the effect of the transfer function. (b) is an observed power spectrum with contributions from several collaborations (Figure from [9]).

2.2.2 Why Fourier space?

Finding out how structure is formed and distributed in the universe is among the great goals of the cosmologist. Yet a precise map of the complete distribution of density fluctuations in the universe (whether it is in position $\delta(\mathbf{x})$ or Fourier space $\delta(\mathbf{k})$), is not only impossible to achieve, but gives us much more information than we need. If we consider a set of identically "created" universes, that is, universes which are governed by the same laws of physics, the density perturbations will not be situated in the exact same positions, nor will they have the same amplitudes. Generating perturbations is a random process, and it tells us nothing about the physics that generated them. What interests us are the overall statistical properties of the density clumps themselves, and this is where the correlation function comes in: From Eq. (2.33) we saw that this function equals the fluctuation variance. Furthermore, rather than considering this mess of variances as a whole, it would be much more practical to look at the statistics scale by scale, that is, constructing a *spectrum* of variances, where each mode in the spectrum is independent of the other.[3] This is what we call the power spectrum.

[3]This is valid only in the case of isotropy, i.e. when the variables do not depend on their orientation.

2.3 The Press-Schechter formalism of large-scale structure formation

The model of spherical collapse can allow us to approximately compute the number density of virialized objects as a function of the mass. The Press-Schechter (PS) model is a model for so-called hierarchical formation of structure. In short, this means that smaller structures will form initially, and that larger structures form by the merging of the smaller ones. Indeed, the hierachical way of structure formation is strongly supported by observations: For example, we observe quasars and galaxies at redshift $z \sim 6$, indicating that small-scale structure was already present when the universe was about 10% of its current age.

The model assumes that the density perturbations have grown sufficiently large that virialized objects are formed. Furthermore, it is assumed that the perturbations initially follow a Gaussian distribution (the following chapter gives further details on this). In practice, this means that the statistical distribution of perturbations with overdensity δ corresponding to a given mass M is given by

$$p(\delta) = \frac{1}{\sigma(M)\sqrt{2\pi}} \exp\left[-\frac{\delta^2}{2\sigma^2(M)}\right]. \tag{2.38}$$

The expectation value of δ is obtained by multiplying it with the distribution and integrating over all values, giving an expression on the form

$$\langle\delta\rangle = \alpha \int_{-\infty}^{\infty} \delta e^{-\beta\delta^2} \mathrm{d}\delta, \tag{2.39}$$

where α, β are constants that can easily be inferred from (2.38). The integrand is an antisymmetric function, so that the integral, and therefore $\langle\delta\rangle$, is zero. We get the expectation value of δ^2 in the same manner, this time by multiplying (2.38) with δ^2 and integrating, which gives

$$\langle\delta^2\rangle = \alpha \int_{-\infty}^{\infty} \delta^2 e^{-\beta\delta^2} \mathrm{d}\delta. \tag{2.40}$$

This type of integral has the solution given as equation (A.9) in Appendix A, and we get

$$\langle\delta^2\rangle = \frac{\alpha}{2\beta}\sqrt{\frac{\pi}{\beta}} = \frac{\sigma^2(M)}{\sqrt{2\pi}\sigma(M)}\sqrt{2\pi\sigma^2(M)} = \sigma^2(M). \tag{2.41}$$

In the PS model, it is assumed that when the perturbations have obtained an overdensity above a critical value δ_c (an example calculation of which was given in Eq. (2.30)), they will quickly collapse into virialized objects with mass M. Further assumptions are made by claiming that the perturbations have a power spectrum $P(k)$ following a power law,

$$P(k) = Ak^{n_s}, \tag{2.42}$$

where A is a normalization constant, and that the background universe is as before described by the EdS model. For fluctuations with a given mass M, the fraction of objects

that are bound at a given epoch is then given by the fraction of perturbations of size larger than $\delta = \delta_c$, from (2.38)

$$F(M) = \alpha \int_{\delta_c}^{\infty} e^{-\beta\delta^2} \mathrm{d}\delta. \tag{2.43}$$

To solve this integral, we apply equations (A.1) and (A.3)–(A.9) in Appendix A. From this, we get

$$\begin{aligned} F(M) &= \beta \left[\frac{1}{2}\sqrt{\frac{\pi}{\beta}} \mathrm{erf}(\sqrt{\beta}\delta) \right]_{\delta_c}^{\infty} \\ &= \frac{\alpha}{\sqrt{\beta}} \left[\int_0^{\sqrt{\beta}\delta} e^{-t^2} \mathrm{d}t \right]_{\delta_c}^{\infty} \\ &= \frac{\alpha}{\sqrt{\beta}} \left(\int_0^{\infty} e^{-t^2} \mathrm{d}t - \int_0^{\sqrt{\beta}\delta_c} e^{-t^2} \mathrm{d}t \right) \\ &= \frac{\alpha}{\sqrt{\beta}} \left(\frac{1}{2}\sqrt{\pi} - \int_0^{\sqrt{\beta}\delta_c} e^{-t^2} \mathrm{d}t \right). \end{aligned}$$

If we substitute the values for α and β, we can write the solution as

$$\begin{aligned} F(M) &= \frac{1}{\sqrt{\pi}} \left(\frac{1}{2}\sqrt{\pi} - \int_0^{\delta_c/\sqrt{2\sigma^2}} e^{-t^2} \mathrm{d}t \right) \\ &= \frac{1}{2}[1 - \mathrm{erf}(t_c)], \end{aligned} \tag{2.44}$$

where we have introduced the new variable

$$t_c = \frac{\delta_c}{\sqrt{2}\sigma}, \tag{2.45}$$

and the error function can be found in the appendix as already mentioned.

The r.m.s. variance in mass on a given scale r, corresponding to the mass M through $r = (3M/4\pi\bar{\rho})^{1/3}$, can be found from the power spectrum by smoothing the density field of scales smaller than r with a window function $W(kr)$:

$$\sigma^2(r) = \int_0^{\infty} \frac{\mathrm{d}k}{k} \Delta^2(k) |W(kr)|^2, \tag{2.46}$$

where $\Delta^2(k)$ was defined in equation (2.37). If the smoothing is a top-hat in real space, it has the Fourier space form

$$W(kr) = \frac{3}{(kr)^3}[\sin(kr) - kr\cos(kr)]. \tag{2.47}$$

An important cosmological parameter is σ_8, the variance in a top-hat region of radius 8 h^{-1}Mpc. The value 8 is pure convention—originally chosen as the approximate scale for

massive galaxy clusters—and is a standard parameter in cosmology for normalizing the matter power spectrum. The newly released 5-year WMAP data, for instance (see ref [10]), constrain $\sigma_8 = 0.796 \pm 0.036$ for our universe.

In order to simplify things as much as possible, we will illustrate by roughly approximating the use of such a window function through writing (2.46) as

$$\sigma^2 \approx \frac{1}{2\pi^2} \int_0^{1/r} P(k) k^2 \mathrm{d}k. \tag{2.48}$$

Since r is the smoothing scale provided by the window function, the upper limit in the integral (2.46) is changed to the approxmate corresponding value of k. It is important to remember that this approximation is merely an illustration for this section, while the more accurate expressions will be used in the modelling to come. From this, and equation (2.42), we solve to get

$$\begin{aligned} \sigma^2 &\approx \frac{A}{2\pi^2} \int_0^{1/r} k^{n_s+2} \mathrm{d}k \\ &= \frac{A}{2\pi^2} \frac{1}{n_s+3} \frac{1}{r^{n_s+3}} \propto r^{-(n_s+3)}. \end{aligned} \tag{2.49}$$

Since the mass contained in a perturbation is proportional to the volume, and therefore $r \propto M^{1/3}$, we can substitute and write

$$\sigma^2 = K M^{-\frac{n_s+3}{3}}, \tag{2.50}$$

where all constants are contained in the new proportionality constant K. We can use this on (2.45) and get an expression that depends on mass:

$$\begin{aligned} t_c &= \frac{\delta_c}{\sqrt{2K}} M^{\frac{n_s+3}{6}} \\ &= \left(\frac{M}{M_*} \right)^{\frac{n_s+3}{6}}, \end{aligned} \tag{2.51}$$

where we have defined $M_* \equiv \left(\frac{2K}{\delta_c^2} \right)^{3/(n_s+3)}$.

The fraction of perturbations with mass in $[M, M + \mathrm{d}M]$ is given by

$$|\mathrm{d}F| = -\frac{\partial F}{\partial M} \mathrm{d}M, \tag{2.52}$$

where the negative sign signifies that F is a decreasing function of M. In the linear regime, $M = \bar{\rho} V$, where $\bar{\rho}$ is the mean density of the EdS universe.[4] As the perturbations became

[4]Remember that the background density equals the critical value, so $\bar{\rho} = \rho_{\mathrm{cr}} = 3H_0^2/8\pi G$.

nonlinear, they continued to collapse until they formed virialized objects with mass M. The number density of such objects then becomes

$$n(M)\mathrm{d}M = -\frac{\bar{\rho}}{M}\frac{\partial F}{\partial M}\mathrm{d}M. \tag{2.53}$$

The quantity $n(M)$ is called the mass function, and it can be calculated for the PS model. To do this, one needs to differentiate and do a couple of tricks, and the derivative of the error function must be known; it is given by equation (A.2). One may then calculate the derivative of F and insert into (2.53) to finally get the expression for the mass function:

$$\begin{aligned}
\frac{\partial F}{\partial M} &= \frac{1}{2}\frac{\partial}{\partial M}\left\{1-\mathrm{erf}\left[\left(\frac{M}{M_*}\right)^{(n_s+3)/6}\right]\right\} \\
&= -\frac{1}{2}\frac{2}{\sqrt{\pi}}\exp\left[-\left(\frac{M}{M_*}\right)^{(n_s+3)/3}\right]\frac{n_s+3}{6}\left(\frac{M}{M_*}\right)^{(n_s-3)/6}\frac{1}{M_*} \\
&= -\frac{1}{2\sqrt{\pi}}\left(1+\frac{n_s}{3}\right)\frac{1}{M_*}\left(\frac{M}{M_*}\right)^{(n_s-3)/6}\exp\left[-\left(\frac{M}{M_*}\right)^{(n_s+3)/3}\right] \\
&= -\frac{1}{2\sqrt{\pi}}\left(1+\frac{n_s}{3}\right)\frac{1}{M}\left(\frac{M}{M_*}\right)^{(n_s+3)/6}\exp\left[-\left(\frac{M}{M_*}\right)^{(n_s+3)/3}\right] \\
\Rightarrow n(M) &= \frac{1}{2\sqrt{\pi}}\left(1+\frac{n_s}{3}\right)\frac{\bar{\rho}}{M^2}\left(\frac{M}{M_*}\right)^{(n_s+3)/6}\exp\left[-\left(\frac{M}{M_*}\right)^{(n_s+3)/3}\right].
\end{aligned} \tag{2.54}$$

To see how this mass function behaves, we finally rearrange (2.54) so that it depends purely on (M/M_*), multiplying both sides by M_*^2:

$$M_*^2 \times n(M) = \frac{1}{2\sqrt{\pi}}\left(1+\frac{n_s}{3}\right)\bar{\rho}\left(\frac{M}{M_*}\right)^{(n_s-9)/6}\exp\left[-\left(\frac{M}{M_*}\right)^{(n_s+3)/3}\right]. \tag{2.55}$$

Figure 2.2 shows the mass function (2.55) for three values of the spectral index n_s.

In litterature, one often encounters the mass function through a slightly different notation. If we introduce the parameter

$$\nu \equiv \frac{\delta_c^2}{\sigma^2(M)}, \tag{2.56}$$

where $\sigma^2(M)$ is as before the r.m.s. variance in the linearly extrapolated distribution of density fluctuations (i.e. the linear power spectrum), smoothed with a tophat filter as described in (2.47), then Eq. (2.44) can be written as $F(M) = \frac{1}{2}(1-\mathrm{erf}\sqrt{\nu/2})$. The mass function can then be expressed as

$$n(M)\mathrm{d}M = \frac{1}{2}\frac{\bar{\rho}}{M}\sqrt{\frac{\nu}{2\pi}}e^{-\nu/2}\frac{\mathrm{d}\nu}{\nu}. \tag{2.57}$$

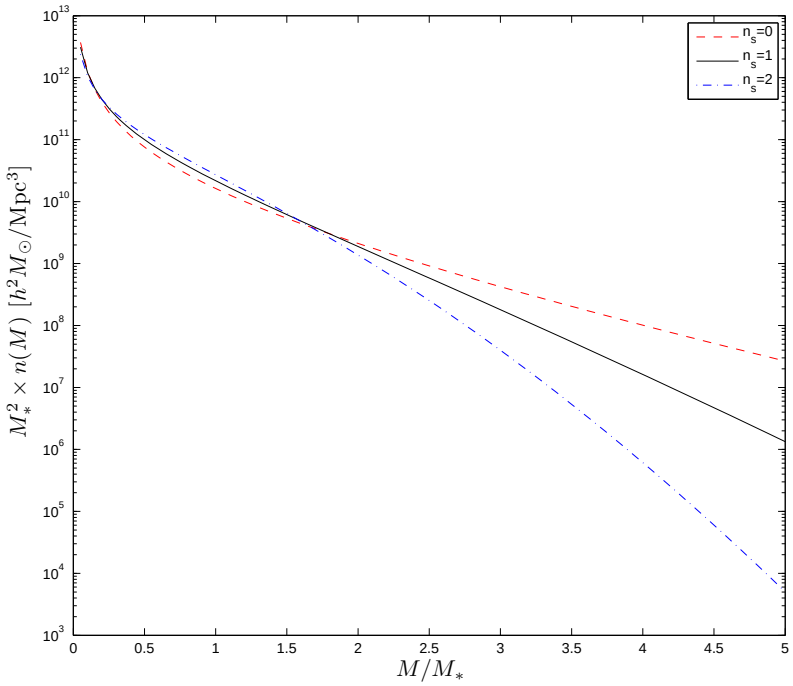

Figure 2.2: Mass function in the Press-Schechter model for three values of the spectral index n_s, showing the tendency of a higher density of perturbations the smaller the mass range. This intuitively comes together with the notion of hierarchical structure formation, where larger mass structures are consecutively formed "on top of" smaller ones. More precisely, this follows from the fact that a larger mass demands a larger smoothing length, and for large mass values the mass function decreases exponentially, as larger mass density peaks become succeedingly rare.

It should be noted that a small detail has so far been left out. A predicament arises in the PS model in that we get the factor 1/2 in front of the right hand side of (2.57). This is a consequence of using a Gaussian field as a starting point for finding the fraction of collapsed overdensities (2.44). Mathematically, Eq. (2.38) gives that half of the universe will then be underdense, and will therefore never exceed the threshold value. This leads to the physically flawed conclusion that only half the universe is able to create bound objects. The solution to this issue was rather ad hoc; Press and Schechter simply multiplied the expression by a factor of two in order to obtain the desired result. Although this would seem a relatively sketchy resort, it nevertheless proceeded to give very good fits to N-body simulation results, and it is in fact through these results that the introduction of the factor 2 is justified.

With this "correcte" PS formalisn in hand, the mass function can now be defined through

$$\frac{M^2}{\bar{\rho}} n(M) \frac{\mathrm{d}M}{M} = \nu f(\nu) \frac{\mathrm{d}\nu}{\nu}, \tag{2.58}$$

where we have introduced the notation

$$\nu f(\nu) = \sqrt{\frac{\nu}{2\pi}} e^{-\nu/2}. \tag{2.59}$$

Note how the mass variable ν and hence $n(M)$ is entirely described by quantities related to linear theory.

A modified version of the form of $f(\nu)$ will later be utilized for the modelling in this thesis.

2.4 Introduction to the neutrino

The neutrino, an elementary particle, was theorized in 1930 by Wolfgang Pauli, as a means to preserve energy and momentum in experiments of β-decay, the decay of a neutron into a proton, an electron and an anti-electron neutrino, written $n \rightarrow p + e^- + \bar{\nu}_e$. Pauli postulated that an unknown particle accounted for the observed difference between the energy, momentum and angular momentum of both sides of the reaction.[5]

Having half-integer spin, the neutrino is therefore a fermion. It is electrically neutral, and hence does not interact through the electromagnetic (or strong) force, only through the weak force as well as gravity. The weakness of the weak force in the interaction of neutrinos with matter makes them exceptionally hard to detect; most neutrinos prefer to pass easily through the entire earth, and to stop only half of them with a wall of lead, it would be quite necessary for the wall to be about a light-year thick. Neutrino detectors are built very massive and with a vast amount of detecting medium, and placed deep under

[5]It was Enrico Fermi who coined the name *neutrino*, as a pun on the italian word for neutron. *Neutrone* seems to use the suffix "-*one*" (allthough this is a coincidence), which indicates something large, whereas "-*ino*" indicates something small.

ground or even ice, to shield them from interference such as cosmic rays. Still, the large flux of neutrinos emanating from the Sun (every second some 10^{11} particles per cm^2 of the one half of the Earth facing the Sun) allows hundreds of them to be detected every year.

2.4.1 Why neutrinos must be massive

There are three known generations (or flavours) of neutrinos: The electron neutrino ν_e, the muon neutrino ν_μ and the tau neutrino ν_τ, named after their connection with the corresponding leptons in decay reactions producing electrons, muons and tau particles, respectively. Each flavour also has a corresponding antiparticle, denoted by a bar $\bar{\nu}$.

It was initially believed that neutrinos were massless particles (actually, in many models this can still be assumed and valid), and a zero mass requires travelling at the speed of light. As mentioned, most neutrinos passing through the Earth come from the Sun, allowing us to detect them. The discovered discrepancy between the number of electron neutrinos detected from the core of the sun and the expected number, known as the Solar Neutrino Problem, was later explained by the neutrinos being able to oscillate between the three flavours. This is a quantum mechanical effect; it occurs because the neutrino flavour eigenstates are different from the neutrino mass eigenstates. Hence there is a certain probability for a neutrino produced in the sun's core as an electron neutrino, to be detected as either a tau or a muon neutrino after having travelled a distance through space. It is evident that the existence of flavour oscillations must imply a non-zero mass: The oscillations between two flavours depend on the difference in the square of their masses.

The first detection of neutrino oscillations, and thus the existence of a non-zero rest mass, were made by the Super-Kamiokande detector as late as 1998, and this was confirmed in several later experiments.

2.4.2 Neutrinos as cosmic inventory

The oscillation experiments on solar and athmospheric neutrinos are only sensitive to the difference in the square of the masses (or mass eigenstates), and we learn nothing of the absolute masses themselves. This is where cosmology comes into play. Cosmology is at present one of the most powerful probes of neutrino properties, since we here get an upper bound for the sum of the absolute neutrino masses.

The early universe was sufficiently hot and dense to serve as a fusion reactor, producing light elements as in the stars of today. Calculations of the reactions in this Big Bang nucleosynthesis (BBN) which formed the light elements show that neutrinos are indeed among the products. So BBN does not only predict the abundance of the light elements in the universe, but also the presence of a sea of cosmic neutrinos. Unlike those originating from the sun, relic cosmological neutrinos have, until recently, not been possible to detect: With the results of the 5-year observation data from the Wilkinson Microwave Anisotropy Probe (WMAP) released March 2008 (see Ref. [10]), one has for the first time found evidence of such a non-zero cosmic neutrino background.

Neutrinos were once kept in equilibrium with the rest of the cosmic plasma, through

interactions such as electron/positron pair production and annihilation, neutrino/antineutrino scattering, and neutrino/electron scattering. For a particle to maintain this equilibrium, the reactions have to occur at a sufficient rate, sufficient meaning it has to remain above the rate of the Hubble expansion $H(t)$. At a certain point, the rates of the weak reactions involving the neutrinos could not keep up with the expansion rate, and about a second after the Big Bang, at a temperature of about 1 MeV or 10^{10} K, the neutrinos decoupled, or "froze out" of equilibrium. The universe continues to cool as it expands, and when it is approximately 3 seconds old, the temperature becomes smaller than about 511 keV. This corresponds to the electron mass, and therefore the threshold for pair production, which means that the electron-positron pairs can no longer be produced efficiently. While production decreases, annihilations continue to take place, and the net result is that the density of e^+e^- pairs decreases fast. The annihilations, written as $e^+ + e^- \rightarrow \gamma + \gamma$. fuels the photon gas with additional energy. While the neutrinos by this time stream freely and out of equilibrium, they do not obtain any of this energy. This in turn means that photons will have a higher temperature after the annihilation period. The temperature ratio can be calculated by requiring conservation of entropy density before and after annihilation. For the case of massless neutrinos, which are always ultrarelativistic, one gets

$$\frac{T_\nu}{T_\gamma} = \left(\frac{4}{11}\right)^{1/3}. \tag{2.60}$$

A current temperature of 2.73 K of the cosmic microwave background (CMB) would therefore gives a neutrino background temperature of $T_\nu \approx 1.95$ K. With a non-zero mass this temperature would have a much lower value.

Table 2.1 sums up the basic features of the neutrino.

Family	Fermion
Group	Lepton
Electric charge	0
Color Charge	0
Spin	1/2
Generations (flavours)	$\{\nu_e, \nu_\mu, \nu_\tau\}$
Antiparticle	$\{\bar{\nu}_e, \bar{\nu}_\mu, \bar{\nu}_\tau\}$
Interaction	Weak force and gravity

Table 2.1: Neutrino fact-sheet.

Cosmological neutrinos are a candidate for so-called hot dark matter (HDM) introduced in Section 2.2, the term 'hot' implying ultra-relativistic thermal velocities at around the time of matter-radiation equality (the particles of cold dark matter (CDM) were non-relativistic at that time).[6] Cosmologists earlier proposed that neutrinos could be the

[6]The relic neutrinos become non-relativistic when the temperature is of order the neutrino mass.

answer to the mysterious identity of dark matter, but constructing models with neutrinos making up all dark matter in the cosmos led to a universe looking radically different from the one we currently live in: The aforementioned free-streaming effect requires that structure formation happened from the "top-down"—large scale structures having formed initially with smaller structures gradually condensing out of the large ones—as opposed to the hierarchical picture mentioned in the last section.

Later on, it has been established that most of the dark matter in the universe is cold (although we have yet to find out what kind of particles CDM consists of). Still, neutrinos can make up a small fraction of the total dark matter density, and there are various methods in cosmology by which we can hope to detect this fraction all the more accurately. One of these methods is to observe the effect a non-zero neutrino density parameter Ω_ν might have on large-scale structure: Because of the free-streaming of massive neutrinos, we may observe less structure on smaller scales of the power spectrum. That is, small-scale density perturbations cannot form for HDM, since (ultra-)relativistic particles are not gravitationally bound to the potential well of an overdensity, and are therefore able to move freely and to escape from the potential well, leading the perturbation to dissolve. In the following chapter, a relatively simple statistical model of large-scale structure is introduced, the *Halo Model*, leaving room to investigate how it may interact with the inclusion of massive neutrinos as a component of dark matter.

Chapter 3

The Halo Model

> for the more limited, if adequate, is always preferable.
>
> —Aristotle (Physics; Book I, Chapter VI)

Chapter 2 presented the Press-Schechter model, an example of an analytical approach for finding the mass function $n(M)$. As mentioned, the mass function is an important quantity describing how gravitationally bound structures are distributed on different mass scales. The PS formalism has successfully and quite accurately described the mass function compared with simulations in the many years since its introduction in 1974, and it was not until the mid-1990s that the precision of simulations had developed enough to show noticable discrepancies, and improving tweaks to the mass function were introduced. The mass function is a naturally important part of the halo model, as we will see in the following sections.

Scientific modelling is about creating a balance between simplicity and concord. In astronomy one may find a complete range of models varying in complexity and accuracy towards observations; the model chosen for this thesis can be said to take a somewhat phenomenological approach, as well as keeping it in a rather simple form. This chapter will attempt to gradually build up a basic understanding of the foundations and ingredients of the halo-based description of non-linear large scale structure.

A large portion of the theory in the chapter is based on the review article by Cooray and Sheth, see Ref. [7], as well as some additional material from [4].

3.1 Origin and concept

3.1.1 Random Fields

A random field is essentially an ensemble of random numbers whose values are mapped on to (an n-dimensional) space. The values in a random field are usually spatially correlated, in the sense that numbers that are further apart generally differ more than the ones that

are adjacent. The field of density contrasts $\delta(\mathbf{x}_i)$ is regarded as a stochastic variable, and thus forms a random field.

Specifically, a *Gaussian random field* is a random field with Gaussian statistics, i.e. involving variables with Gaussian probability density functions like the one in Eq. (2.38). The conventional assumption in cosmology is that the initial distribution set up by inflation—the primordial density field—is Gaussian. The important part is that if the statistical properties of the density field are Gaussian, then they are uniquely characterized by its two-point correlation function $\xi(r)$, or equivalently, the power spectrum $P(k)$ (Eqs. (2.35) and (2.37)).

3.1.2 The model

The foundation for the halo model originates over half a century ago, through the studies of the spatial distribution of galaxies led by Jerzy Neyman and Elizabeth Scott, see Ref. [11]. Neyman and Scott thought of the galaxies as a distribution of discrete clusters of various sizes, and hence it followed that it was natural to study this distribution by its statistical properties, since the clusters now were viewed as discrete points.

Up until the recent years, and through many new discoveries about the constituents and behaviour of the universe, advanced and detailed numerical simulations have been developed, studying the large-scale non-linear evolution of the distribution of dark matter. Starting with an initially smooth distribution containing small perturbations, a complex structure evolves, consisting of features such as filaments, voids and dense knots. The knots are often called dark matter halos.

The concept of the halo model is that all matter in the universe is entirely confined to halos of different size and mass, illustrated in Figure 3.1. If individual halos can be

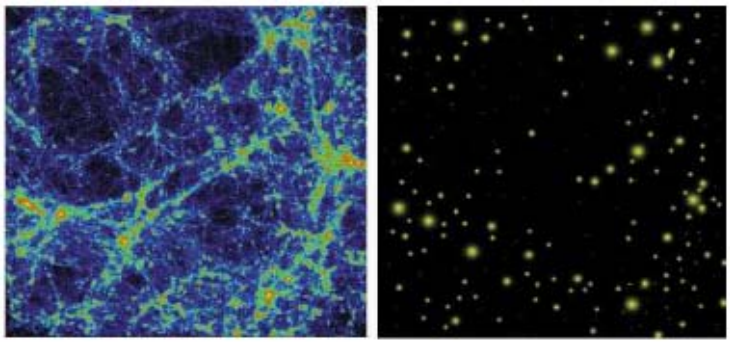

Figure 3.1: This figure illustrates how the complex features found in numerical simulations of the dark matter distribution (left panel) can be replaced by dark matter halos (right panel). Illustration taken from [7].

identified, then one assumes that the halos are small compared to the distance between them. From this comes the important key to the model, that the mass distribution can be studied in two steps:

1. On small scales (smaller than the size of a typical halo), the statistics of the density field are determined by the spatial distribution within the halos; how the halos themselves are distributed in space is not important.

2. On large scales (larger than the size of a typical halo), it is the spatial distribution of the halos that becomes important, and the internal details of a halo become insignificant.

What the model assumes is that the actual physics can be thought of in two steps as well as the statistics. The halos are furthermore approximated to be in virial equilibrium, so that the definition of a halo is essentially a region which has become sufficiently overdense with respect to the background that it has collapsed. The spherical collapse model introduced in the previous chapter will serve as the mechanism for such collapse in the thesis.

3.2 Formalism and ingredients

3.2.1 The power spectrum of dark matter

In the previous chapter, through the Press-Schechter formalism of spherical collapse, it was demonstrated that predictions from linear theory is used to describe the mass function (2.58): The mass variable ν is defined as the squared ratio of the predicted linear theory value of the density contrast of a spherically collapsing region, denoted δ_c, and the rms variance $\sigma(M)$ of the linear power spectrum, smoothed with a top-hat window function on scale r, corresponding to a mass M. Some of the statistical description of random fields were introduced in section 2.2, where Fourier space was introduced as a useful environment in which to look at cosmic structure.

We will work exclusively in Fourier space when describing the halo model. This is convenient because the correlation function involves convolutions, which simply transcribe as ordinary multiplications when Fourier transformed. The power spectrum of dark matter in the halo model is written as mentioned in two parts:

$$P_{\rm dm}(k) = P^{\rm 1h}_{\rm dm}(k) + P^{\rm 2h}_{\rm dm}(k) \tag{3.1}$$

where

$$P^{\rm 1h}_{\rm dm}(k) = \int {\rm d}M n(M) \left(\frac{M}{\bar{\rho}}\right)^2 |u(k|M)|^2, \tag{3.2}$$

$$P^{\rm 2h}_{\rm dm}(k) = \int {\rm d}M_1 n(M_1) \left(\frac{M_1}{\bar{\rho}}\right) u(k|M_1) \times \int {\rm d}M_2 n(M_2) \left(\frac{M_2}{\bar{\rho}}\right) u(k|M_2) P_{\rm hh}(k|M_1, M_2), \tag{3.3}$$

where the first term describes the correlations within one halo—the non-linear, intra-halo regime—and the second term describes the correlation between two different halos—the

(quasi-)linear, inter-halo regime. Here $\bar{\rho}$ is the mean background density of the universe, and $n(M)$ is the previously discussed mass function of the virialized dark matter halos. The remaining factors which build up equations (3.2) and (3.3) will be explained in the following subsections.

3.2.2 Halo bias and the linear dark matter power spectrum

Halos are biased tracers of the overall dark matter content. The above expression comes from the defined form of the overdensity of a halo residing in a cell of comoving volume V:

$$1 + \delta_h(m, z|M, V, z_0) = \frac{\bar{N}(m, z|M, V, z_0)}{n(m, z)V}. \tag{3.4}$$

Here, $\bar{N}(m, z|M, V, z_0)$ stands for the average number of halos of mass m which collapsed at time z, situated in cells of size V containing mass M at time z_0. The previously discussed mass function is in the denominator. Rewriting the number of halos as

$$\bar{N}(m, z|M, V, z_0) = n(m, z, |M, V, z_0) = n(m, z|M, V, z_0)V(1 + \delta), \tag{3.5}$$

where $V(1 + \delta) = M/\bar{\rho}$ is the initial comoving size of the now overdense region V, an expression for $n(m, z|N, V, z_0)$ can be found. It is explained in [7] that there is a direct relation between the actual matter overdensity δ and the linearly extrapolated prediction δ_0, such that $\delta_0 = \delta_0(\delta, z_0)$. At the same time remembering that the mass function depends on the linear prediction of the overdensity at spherical collapse $\delta_c(z)$, the right hand side of (3.5) can be approximated by letting it depend on $\delta_c(z) - \delta_0(\delta, z_0)$.[1] One may then estimate the density of halos of mass m, having virialized at z and being inside cells of size V with mass M at z_0, as

$$\frac{m^2 n(m, z|M, V, z_0)}{\bar{\rho}} \frac{\mathrm{d}m}{m} = \nu_{10} f(\nu_{10}) \frac{\mathrm{d}\nu_{10}}{\nu_{10}}, \tag{3.6}$$

where

$$\nu_{10} \equiv \frac{[\delta_c(z) - \delta_0(\delta, z_0)]^2}{\sigma^2(m) - \sigma^2(M)}. \tag{3.7}$$

If $V \to \infty$, then $M \to \infty$, and $\sigma^2(M)$ and $|\delta|$ tend towards zero, reducing the expression to the mass function (2.58). Looking at the large cell limit, such that $\sigma^2(M) \ll 1$, then $|\delta| \ll 1$ and we can use a power expansion in small δ for $\delta_0(\delta, z_0)$, on the form $\delta_0/(1+z) = \sum_{k=0}^{\infty} a_k \delta^k$. Since the mass M in large cells is itself large, then $\sigma(M) \ll \sigma(m)$ for most values of m, such that $\sigma(M) \to 0$. The expression for $n(m, z|M, V, z_0)$ can thus be expanded on the form

$$n(m, z|M, V, z_0) \approx n(m, z) - \delta_0(\delta, z_0) \left(\frac{\partial n(m, z)}{\partial \delta_c} \right)_{\delta_c(z)}; \tag{3.8}$$

[1] The value δ in itself can not be used in this case, as $\delta_c(z)$ has been derived through extrapolating it using linear theory, and the actual value δ has been derived non-linearly.

which in turn gives

$$\delta_h(m, z|M, V, z_0) \approx \delta - (1+\delta)\delta_0(\delta, z_0) \left(\frac{\partial \ln n(m,z)}{\partial \delta_c} \right)_{\delta_c(z)}. \tag{3.9}$$

With this, and a suitable form of the mass function $n(m, z)$, it can be shown that keeping terms to lowest order in δ, yields a bias relation

$$\delta_h(m, z|M, V, z_0) \approx b(m, z)\delta. \tag{3.10}$$

That is, the overdensity of dark matter halos in very large cells is linearly proportional to the overdensity of the mass, and the constant of proportionality depends only on halo mass and the redshift at which the halo collapsed into a virialized object (it does not depend on cell size).

Note that it was necessary in this discussion of the development of the halo overdensity relative to that of matter to include redshift, where as this thesis will concentrate on the case $z = 0$. The bias relation will then only depend on halo mass.

For the most massive halos, $b(m) \gg 1$, meaning that they therefore occupy the densest cells. In a Gaussian random field, the densest regions are more strongly clustered than those of average density (see e.g. [12]). Another way of saying this is that the correlation function of a dense fluctuation field (e.g. that of a rich cluster of galaxies) has a higher value. Remembering the definition of the power spectrum (2.35), a reasonable approximation to the halo-halo power spectrum in (3.3) on large scales is therefore to relate it to the overall dark matter spectrum via the linear bias $b(m)$:

$$P_{\rm hh} = b_1(M_1)b_2(M_2)P_{\rm dm}(k). \tag{3.11}$$

Since correlations on between halos are only important on the large, quasi-linear scales, Eq. (3.11) may further be approximated by setting $P_{\rm dm}(k) \approx P^{\rm lin}_{\rm dm}(k)$, the linear dark matter power spectrum.

3.2.3 Radial density profiles of halos

A good description of the radial density profile of the dark matter contained in virialized halos is given by a function of the form

$$\rho(r|M) = \frac{\rho_s}{(r/r_s)^\alpha (1 + r/r_s)^\beta}. \tag{3.12}$$

If we set $\alpha = 1$ and $\beta = 2$, we get the NFW (Navarro-Frenk-White [13]) profile, which has acted as a very good description of the density profile in numberical simulations, and which is the profile considered for this thesis,[2]

$$\rho(r|M) = \frac{\rho_s}{r/r_s(1 + r/r_s)^2}. \tag{3.13}$$

[2] (α, β)=(1,3) gives the Hernquist profile whereas $\rho = \rho_s/[(r/r_s)^\alpha(1 + (r/r_s)^\beta)]$ with (α, β)=(3/2,3/2) gives the M99 profile [14, 15].

Here, r_s is a characteristic scale radius, which in turn defines a scale density ρ_s. The scale radius is determined by what gives the best fit to the density profile, when given an object of mass M and the corresponding *virial radius* (i.e. what defines the edge of a virialized object), which is a function of the mass:

$$r_{\rm vir} = \left(\frac{3M}{4\pi \Delta_{\rm vir} \bar{\rho}} \right)^{1/3}. \tag{3.14}$$

From this, we can say that the virial radius is the radius enclosing a virialized spherical object with density contrast $\Delta_{\rm vir}$, and $\bar{\rho}$ being the background density of the universe.

The combination of r_s and the mass M, which can be calculated as

$$M = 4\pi \int_0^{r_{\rm vir}} {\rm d}r \, r^2 \rho(r|M), \tag{3.15}$$

then gives the amplitude ρ_s. For the NFW profile, Eq. (3.15) gives

$$M = 4\pi \rho_s r_s^3 \left[\ln(1+c) - \frac{c}{1+c} \right] \equiv 4\pi \rho_s r^3 g(c), \tag{3.16}$$

where the *concentration parameter* $c \equiv r_{\rm vir}/r_s$.

The normalized Fourier transform of the density profile is obtained through

$$u(k|M) = 4\pi \int_0^{r_{\rm vir}} {\rm d}r \, r^2 \frac{\sin(kr)}{kr} \frac{\rho(r|M)}{M}. \tag{3.17}$$

For the NFW profile, one gets

$$\begin{aligned} u(k|M) \;=\; & \frac{4\pi \rho_s r_s^3}{M} \Big\{ \sin(kr_s) \left[{\rm Si}([1+c]kr_s) - {\rm Si}(kr_s) \right] - \frac{\sin(ckr_s)}{(1+c)kr_s} \\ & + \cos(kr_s) \left[{\rm Ci}([1+c]kr_s) - {\rm Ci}(kr_s) \right] \Big\}, \end{aligned} \tag{3.18}$$

where the sine and cosine integrals ${\rm Si}(x), {\rm Ci}(x)$ are defined in Appendix A through Eqs. (A.6) and (A.7).

3.3 The galaxy distribution within dark matter halos

It is known that galaxies of different type cluster in different ways, meaning that they do not trace the underlying mass in an exact manner. This relation between the distribution of galaxies and dark matter is called the galaxy bias, and it is thus said that galaxies are *biased tracers* of the overall matter distribution. We will now have a look at the manner in which the clustering of galaxies can be inferred, based on the description of that of dark matter, which has already been presented.

An important part of the transition from the power spectrum of dark matter and that of galaxies is the assumption that in the model, galaxies can only form within halos. The equations for the power spectrum are then weighted by the number of galaxies per halo (depending on halo mass), rather than by the mass of the underlying dark matter particles. This is utilized through what is called the halo occupation distribution (HOD). The first moment of the HOD, the mean halo occupation number $\langle N|M\rangle$, governs the galaxy clustering on inter-halo scales, while the intra-halo term aquires the second HOD moment $\langle N(N-1)|M\rangle$. We then write

$$P_{\rm gal}(k) = P^{\rm 1h}_{\rm gal}(k) + P^{\rm 2h}_{\rm gal}(k), \tag{3.19}$$

where

$$P^{\rm 1h}_{\rm gal}(k) = \int {\rm d}M n(M) \frac{\langle N(N-1)|M\rangle}{\bar{n}^2_{\rm gal}} |u_{\rm gal}(k|M)|^p, \tag{3.20}$$

$$P^{\rm 2h}_{\rm gal}(k) = P^{\rm lin}_{\rm dm}(k) \left[\int {\rm d}M n(M) b(M) \frac{\langle N|M\rangle}{\bar{n}_{\rm gal}} u_{\rm gal}(k|M)\right]^2. \tag{3.21}$$

Here the mean number density of galaxies is

$$\bar{n}_{\rm gal} = \int {\rm d}M n(M) \langle N|M\rangle, \tag{3.22}$$

and $u_{\rm gal}(k|M)$ is the normalized fourier transform of the galaxy density profile, again noting that galaxies are considered rather than dark matter. A reasonable assumption is that galaxies trace the dark matter in such a way that one can utilize the dark matter density profile in the model, e.g. the NFW profile, and this profile will indeed be assumed in this thesis. Therefore, we set $u_{\rm gal}(k|M) = u(k|M)$, given by Eq. (3.18). Furthermore, the simplest model is to take $p = 2$ in (3.20). Note also that correlations between two halos of different masses are no longer assumed, as in the general form (3.3), further simplifying the expression.

On large scales, the two-halo term dominates, and $u_{\rm gal} \to 1$. The integral in Eq. (3.21) is therefore independent of scale, and the galaxy power spectrum simplifies to

$$P_{\rm gal}(k) \overset{k\to 0}{\approx} P^{\rm 2h}_{\rm gal}(k) = b^2_{\rm gal} P^{\rm lin}(k) \tag{3.23}$$

where the mean galaxy bias factor is introduced as

$$b^2_{\rm gal} \equiv \int {\rm d}M n(M) b(M) \frac{\langle N|M\rangle}{\bar{n}_{\rm gal}}. \tag{3.24}$$

Armed with some of the technical information on the constituents of the halo model, the next step will be to implement it in a suitable fashion, i.e. modelling the galaxy power spectrum.

Chapter 4

Method

> Profanity is the one language understood by all programmers.
>
> —Anon.

This chapter presents the chosen way of modelling used for this thesis. The first section describes which forms will be used for the ingredients introduced in the previous chapter. Next, a short explanation will be given for the role of massive neutrinos in the halo model and how this can be implemented in an as simple way as possible.

The integrals (3.20) and (3.21) are not trivial, and therefore they need to be solved numerically. Section 4.3 will briefly go through the structure of the written program which is used to produce numerical results, the code of which is also presented in Appendix B.

In modelling the galaxy power spectrum of the halo model, it is desirable to make the simplest theoretical approaches, and at the same time rely on several empirical data. These data are chosen from the article by Collister & Lahav, see Ref. [16]. Numerical fits for the transfer function and necessary modifications, as well as the mass variance $\sigma(M)$, are also taken from litterature; see text for references.

4.1 Modelling the galaxy power spectrum

4.1.1 The mass function

Remembering Equation (2.58) and the definition (2.56), the mass function will be computed in the form

$$n(M) = \frac{\bar{\rho}}{M}\nu f(\nu)\frac{1}{\nu}\frac{\mathrm{d}\nu}{\mathrm{d}M}, \tag{4.1}$$

where a modified version of the PS formalism will be used, developed by Sheth & Tormen in 1999 from N-body simulations (see Ref [17]), written

$$\nu f(\nu) = A_* \left[1 + (q\nu)^p\right] \left(\frac{q\nu}{2\pi}\right)^{1/2} e^{-q\nu/2}. \tag{4.2}$$

Here A_* is a normalization constant to make the integral of $f(\nu)$ over all ν equal unity. Setting $\{A_*, p, q\} = \{1/2, 0, 1\}$ will retrieve the Press-Schechter formula (2.59). The fitted parameters in the Sheth-Tormen formalism are

$$\begin{aligned} A_* &= \left(1 + \frac{2^{-p}\Gamma\left(\frac{1}{2} - p\right)}{\sqrt{\pi}}\right)^{-1} \approx 0.3222, \\ p &= 0.3, \\ q &= 0.707. \end{aligned}$$

In order to be able to model the mass function in a rather simple manner, a little preliminary analytical work needs to be done. For the variance in mass of the linear dark matter power spectrum will be used a parametrization from [18], based on numerical fitting on results based on the transfer function which will be introduced shortly:

$$\sigma(M) = \sigma_8 \left(\frac{M_*}{M}\right)^{(0.3\Gamma+0.2)/3}. \tag{4.3}$$

The threshold value M_* is set to be the mass of a spherical area with density $\bar{\rho}$ and radius 8 h^{-1}Mpc. For example, setting the background density to be that of a spatially flat universe, gives $M_* \simeq 6 \times 10^{14}\, h^{-1} M_\odot$. The standard mass variance σ_8 was introduced in Section 2.3, whereas the shape parameter is $\Gamma = \Omega_m h$ (not to be confused with the gamma function already mentioned), showing the dependence on cosmology of $\sigma(M)$ and therefore also the mass function.

First calculating $\mathrm{d}\nu/\mathrm{d}M$ by using Eqs. (2.56) and (4.3), one obtains

$$\begin{aligned} \frac{\mathrm{d}\nu}{\mathrm{d}M} &= \delta_c^2 \frac{\mathrm{d}}{\mathrm{d}M}\sigma^{-2}(M) = -2\delta_c^2 \sigma^{-3}(M) \frac{\mathrm{d}\sigma(M)}{\mathrm{d}M}; \\ \frac{\mathrm{d}\sigma(M)}{\mathrm{d}M} &= \sigma_8 \left[-\frac{0.3\Gamma + 0.2}{3}\right] M_*^{(0.3\Gamma+0.2)/3} M^{-(0.3\Gamma+0.2)/3} M^{-1} \\ &= \left[-\frac{0.3\Gamma + 0.2}{3}\right] M^{-1}\sigma(M); \\ \Rightarrow \frac{\mathrm{d}\nu}{\mathrm{d}M} &= \frac{2\delta_c^2[0.3\Gamma + 0.2]}{3\sigma^2(M)M} = \frac{2\nu[0.3\Gamma + 0.2]}{3M}. \end{aligned} \tag{4.4}$$

Finally dividing by ν to get $(1/\nu)(\mathrm{d}\nu/\mathrm{d}M) = [2(0.3\Gamma + 0.2)]/3M$, the following expression for (4.1) can be implemented:

$$n(M) = \frac{2[0.3\Gamma + 0.2]}{3} \frac{\bar{\rho}}{M^2} \nu f(\nu). \tag{4.5}$$

4.1.2 Halo bias function

The halo bias function in Eq. (3.21) depends on the form of the mass function. For the halo bias, which also depends on mass, the form derived by Sheth & Tormen is

$$b(M) = 1 + \frac{q\nu - 1}{\delta_c} + \frac{2p/\delta_c}{1 + (q\nu)^p}, \tag{4.6}$$

where q, p, δ_c and ν are defined as before.

4.1.3 Halo occupation distribution

A simple approach to describing the mean halo occupation number $\langle N|M\rangle$ is by letting it behave as a power law on the form

$$\langle N|M\rangle = \left(\frac{M}{M_0}\right)^{\beta} \tag{4.7}$$

where the free parameters are fitted by Collister & Lahav using the 2dFGRS galaxy catalogue as $\beta = 0.99$ and $\log(M_0/h^{-1}M_\odot) = 13.5$. The second moment $\langle N(N-1)|M\rangle$ is usually expressed via the parameter $\alpha(M)$, such that

$$\langle N(N-1)|M\rangle = \alpha^2(M)\langle N|M\rangle^2. \tag{4.8}$$

In the modelling we will assume that the halos are poisson distributed, which gives $\alpha(M) = 1$. Therefore,

$$\langle N(N-1)|M\rangle \simeq \left(\frac{M}{M_0}\right)^{2\beta}. \tag{4.9}$$

For the mean number density of galaxies, defined in Eq. (3.22), the value derived by Collister & Lahav is

$$\bar{n}_{\rm gal} = 5.06 \times 10^{-3} h^3 \ {\rm Mpc}^{-3}.$$

4.1.4 Fourier-transformed density profile

The NFW density profile will as mentioned be used for the modelling, and the normalized Fourier transformed expression for this profile was given by Eq. (3.18). The concentration parameter c of dark matter halos in simulations is found to be a slightly decreasing function of mass, modelled as a power law on the form $c = c_0(M/M_*)^{-\lambda}$, with $\lambda \sim 0.1$ and $c_0 \sim 10$, and M_* being the value of the mass at which $\nu = 1$. (e.g. [19]). Collister & Lahav measured and found a slight decrease with mass, but there is only a barely significant trend. Therefore we will here implement the mean value independent of mass, fitted by Collister & Lahav to be $c = 2.4$.

The scale radius was defined through the virial radius in Eq. (3.14) and the concentration parameter $c = r_{\rm vir}/r_s$, giving

$$r_s = \left(\frac{3M}{4\pi\Delta_{\rm vir}\bar{\rho}c^3}\right)^{1/3}. \tag{4.10}$$

Inserting this into (3.18), gives

$$u_{\rm gal}(k|M) = \frac{1}{g(c)}\Big\{\sin(kr_s)\left[\mathrm{Si}([1+c]kr_s)-\mathrm{Si}(kr_s)\right]-\frac{\sin(ckr_s)}{(1+c)kr_s} + \cos(kr_s)\left[\mathrm{Ci}([1+c]kr_s)-\mathrm{Ci}(kr_s)\right]\Big\}, \tag{4.11}$$

where

$$g(c) \equiv \ln(1+c) - \frac{c}{1+c}. \tag{4.12}$$

The collapse overdensity is set to $\Delta_{\rm vir} = 200$, a common convention. Lastly, existing numerical routines to compute the sine and cosine integrals (A.6) and (A.7), taken from [20], will be utilized.

4.1.5 Linear dark matter power spectrum

In order to compute the 2-halo term of the galaxy power spectrum, the linear power spectrum for the dark matter needs to be used in some form. We will use the scale invariant ($n_s = 1$) form of Eq. (2.36),

$$P_{\rm dm}^{\rm lin}(k) = AkT^2(k), \tag{4.13}$$

where a fitted form of the transfer function taken from [21] will be implemented:

$$T(k) = \frac{\ln(1+d_1k/\Gamma)/(d_1k/\Gamma)}{\left[1+d_2k/\Gamma+(d_3k/\Gamma)^2+(d_4k/\Gamma)^3+(d_5k/\Gamma)^4\right]^{0.25}}. \tag{4.14}$$

Here the shape parameter is $\Gamma = \Omega_m h$, and values of the coefficients d_1 through d_5 can be found in table 4.1.

The power spectrum will also have to be normalized, in order to fit with the chosen value of σ_8, which will be a free input parameter. Remember that this mass variance was given by

$$\sigma_8^2 = \frac{1}{2\pi^2}\int_0^\infty \mathrm{d}k k^2 W(kr)^2 AkT^2(k), \tag{4.15}$$

where $r = 8h^{-1}$ Mpc and the window function was a top-hat filter. In order to get the right value with the chosen $\sigma(M)$ and σ_8, we compute the integral above with $P_{\rm dm}^{\rm lin}(k) = kT^2(k)$, square it and divide by the input value of σ_8^2. The correct normalization constant A of the linear power spectrum is thus obtained.

4.2 Extension of the model to include massive neutrinos

As mentioned in Chapter 2, massive neutrinos comprising a part of the dark matter is expected to suppress the power spectrum on small scales, a consequence of the free-streaming

effect. In the simple form of the halo model investigated here, the effect of massive neutrinos will come into play through a modification of the linear power spectrum. This modification due to non-zero neutrino mass will be computed as

$$P^{\rm lin}_{{\rm dm}+\nu}(k) = P^{\rm lin}_{\rm dm}(k) f_{\Omega_\nu}(k), \tag{4.16}$$

where a form of the massive neutrino addition from [22] will be used:

$$f_{\Omega_\nu}(k) = \left(\frac{1 + e_1 (k/\Gamma_\nu)^{e_4/2} + e_2 (k/\Gamma_\nu)^{e_4}}{1 + e_3 (k/\Gamma_\nu)^{e_4}} \right)^{\Omega_\nu^{1.05}}. \tag{4.17}$$

The best-fit coefficients can be found in table 4.1. The shape parameter is given by $\Gamma_\nu = \Omega_\nu h$, the density parameter for massive neutrinos is Ω_ν, and the total mass of the three neutrino generations are connected by the expression

$$\Omega_\nu h^2 = \frac{\sum m_\nu}{93.14\,{\rm eV}}. \tag{4.18}$$

This expression is valid for neutrinos each having mass less than about 1 MeV.

d_1	2.34	d_4	5.46
d_2	3.89	d_5	6.71
d_3	16.1		
e_1	0.004321	e_3	11.63
e_2	2.217×10^{-6}	e_4	3.317

Table 4.1: Fitted coefficients for the modelling of the transfer function, with inclusion of massive neutrinos. Parameters d_1–d_5 and e_1–e_4, are for Eqs. (4.14) and (4.17), respectively.

The conclusion one can draw based on what is used in the model, is that massive neutrinos will affect only the 2-halo term (3.21) through the linear power spectrum of dark matter. Because of the free-streaming effect, any damping of the galaxy power spectrum through these functions is expected to occur at small scales.

4.3 Structure of the program

The galaxy power spectrum in the halo model is constructed by means of writing a program package using the FORTRAN90 language. The first part of this package is a main program, in which we carry out the main calculations, including integration and writing to files which can later be studied through plots. The second part is a utility module for stacking all the different routines and parameters concerning the calculation of the different parts of the power spectra in the main program, such as the mass function and the linear dark matter

Description	Symbol	Value
Mean galaxy number density	$\bar{n}_{\rm gal}/(h^3{\rm Mpc}^{-3})$	$(5.06 \pm 0.49) \times 10^{-3}$
Best fit parameters for the	β	$0.99^{+0.15}_{-0.17}$
HOD expectation values	$\log(M_0/h^{-1}M_\odot)$	$13.5^{+0.13}_{-0.19}$
Concentration parameter	c	2.4 ± 0.2
Mean background density	$\bar{\rho}/(h^2 M_\odot{\rm Mpc}^{-3})$	2.775×10^{11}
Matter density parameter	Ω_m	0.3
Hubble constant	h	0.7

Table 4.2: Values held constant when modelling the galaxy power spectrum in the halo model. The fitted values in the first three rows are empirical and taken from [16]. Uncertainties for $\bar{n}_{\rm gal}$ and c are 1-σ. The NFW density profile is assumed, and the background density is taken to be that of a spatially flat universe.

spectrum. It also contains two routines from [20]: one that calculates the sine and cosine integrals used in Eq. (3.18), and one for making abcissas and weights for Gauss-Legendre Quadrature, the chosed integration method (see Appendix B.1 for a short description). A routine for reading some variable input parameters from a text file is also included in the utility module. Lastly there is a module with definitions of kind types and mathematical constants for use in double precision. This last module can be found in [23].

Source code for the program package with notes and comments can be found in its entirety in Appendix B.2.

Chapter 5

Results and discussion

> The most exiting phrase to hear in science, the one that heralds the most discoveries, is not "Eureka!" but "That's funny..."
>
> —Isaac Asimov

This chapter, which presents and discusses the results from some of the modelling described in the Chapter 4, is divided into two main parts. The first part shows some basic results on the halo model when applying the functions and parameter values from Section 4.1. Thereafter, the effects on the galaxy power spectrum from the inclusion of massive neutrinos will be discussed, as well as considering an additional modification.

5.1 Without massive neutrinos

To begin with, in Figure 5.1, the functions which make up the 1-halo and 2-halo terms of the galaxy power spectrum are plotted, using the values in Table 4.2 and setting $\sigma_8 = 0.8$. The r.m.s. variance of the linear power spectrum, Eq. (4.3), is plotted in Figure 5.1(a), showing the simplified power law form. The mass function (4.5) is shown in Figure (b). In Figure (c) the mean halo occupation number, on the form (4.7), is plotted along with the halo bias function (4.6). Figure 5.2 shows the output of the Fourier transformed halo density profile, assuming the NFW form, for a range of masses.

Moving on to the power spectra, one can see in Figure 5.3 the linear power spectrum of dark matter, from Eq. (4.13) and with the transfer function (4.14). The total galaxy power spectrum $\Delta^2_{\rm gal}(k) = \Delta^2_{\rm 1h}(k) + \Delta^2_{\rm 2h}(\rm k)$ can be found in Figure 5.4, together with the two terms plotted separately. The linear power spectrum is also shown, to demonstrate that the galaxy power spectrum is linear at large scales.

A mention of a notable feature of the halo model is in order. If only overdense perturbations are considered (as is the case in the form of the model already discussed), the 1-halo term does not behave as it should. Looking at Eq. (3.2), the weakness of the model

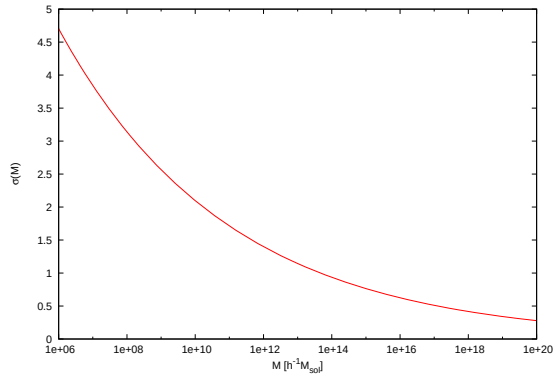

(a) The r.m.s. variance of the linear density fluctuations

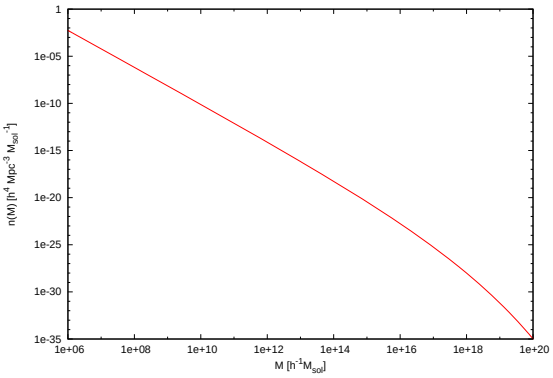

(b) The mass function in the halo model

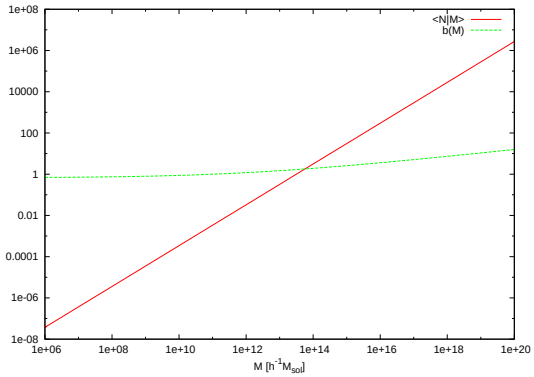

(c) A plot of the mean halo occupation number $\langle N|M\rangle$, together with the halo bias function, which is a slowly increasing function of mass, with lower mass halos being antibiased ($b < 1$).

Figure 5.1: Constituents of the halo model depending on mass

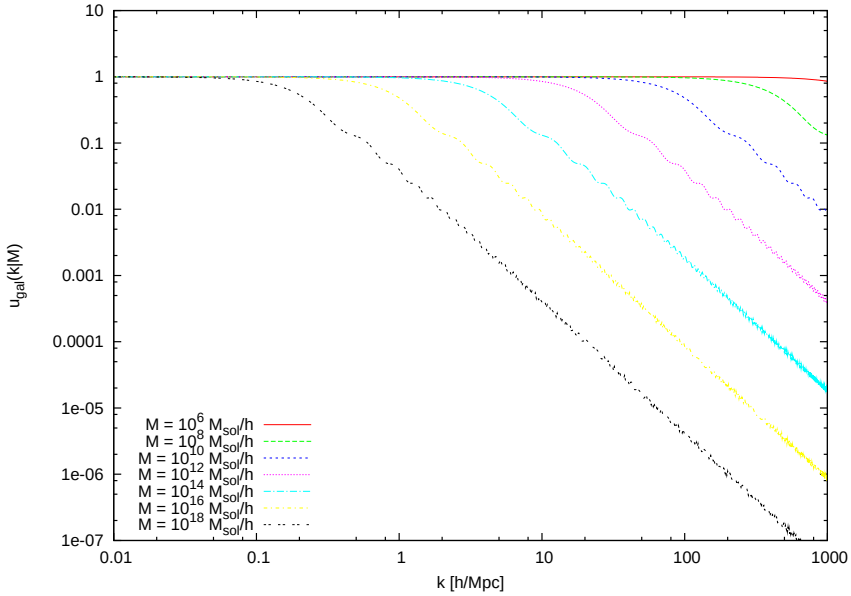

Figure 5.2: The Fourier transformed NFW density profile of halos (Eq. (3.18)), plotted as a function of scale k for several values of halo mass. When the mass of the halo is smaller, it contributes to the total power on smaller and smaller scales, while the largest halos only contribute on large scales.

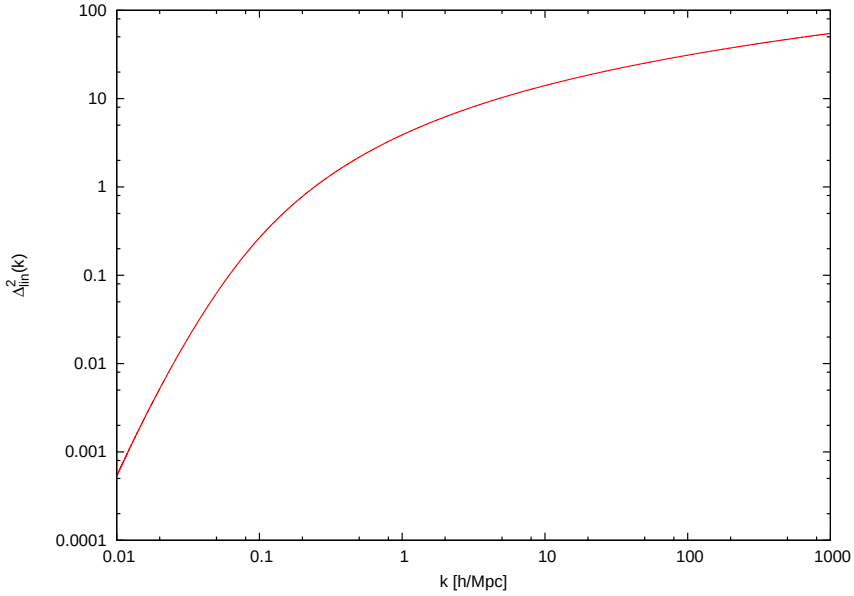

Figure 5.3: The linear power spectrum of dark matter.

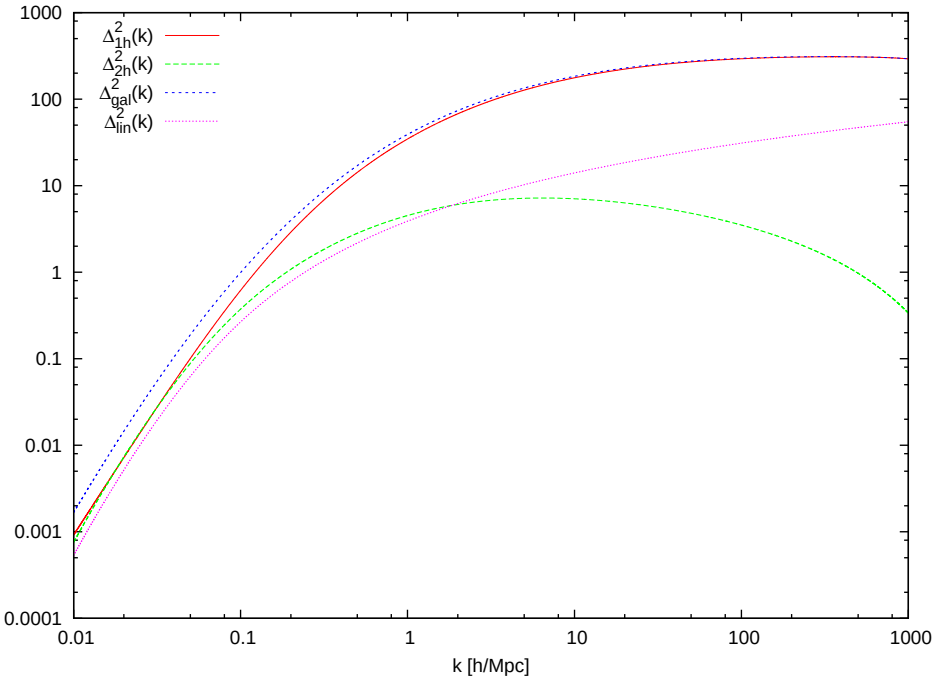

Figure 5.4: The power spectrum of the galaxy distribution in the halo model, shown both as the total and the two separate terms. The linear power spectrum is included for reference.

lies in that as $k \to 0$, the intra-halo power tends to a constant, namely

$$P^{1h}(k \to 0) \to \int \mathrm{d}M n(M) \left(\frac{M^2}{\bar{\rho}^2} \right). \tag{5.1}$$

The actual behaviour of a non-linear power spectrum on the largest scales would be that it turns to zero, at a faster rate than the linear term which scales as k, which would in reality dominate. This weakness, that the 1-halo term seems to dominate over the linear term at small k, is discussed in [7]. Methods of compensated density profiles (i.e. compensating for both over- and underdense regions) and other ways to remove the large scale intra-halo power, are mentioned. However, it is not a simple task, as the density profiles play a part in both terms, and moreover, such compensations will actually lead to vanishing power at small scales, a feature which does not improve the model overall. The weakness of the large-scale limit of the 1-halo term has been treated as an open question. However, the ultimate goal of this thesis is to look at scales below the troublesome threshold, so the problem will not play a significant part in this chapter.

Looking back at Figure 5.4, note that the power spectrum is completely dominated by the 1-halo term throughout the graph, not seeming to let the 2-halo term dominate on the linear scales. This is an indication of the problem mentioned in the previous paragraph. Also, since the small scales are the ones that are interesting for this thesis, and massive neutrinos will play a role only in the 2-halo term, the large dominance of $P^{1h}(k)$ could be a possible issue when examining the effect on the power spectrum of adding neutrino mass.

5.2 Including massive neutrinos

The HDM density parameter Ω_ν is varied to look at the effects on small scales of different values of the total neutrino mass. The scales of interest which still hold physical relevance towards large scale structure cosmology, would lie in the area $k \in [0.1, 1]$; refer back to Figure 2.1(b). Due to the fact that the 1-halo term, which in this model is unaffected by neutrinos, dominates the power spectrum on the smaller scales, it may be that the total power spectrum will in turn lack a visible effect from neutrinos. Figure 5.5 indicates that there seems indeed to be very little damping at small scales.

As a side note, in Figure 5.6 is shown the galaxy power spectrum, but this time for $\sigma_8 = 0.6$. This value makes the relationship between the two terms in the halo model more distinct and intuitive, and the 1h-term is also shifted toward a seemingly more reasonable form on the larger scales. Nevertheless, adding massive neutrinos in this case will still not affect the total power on the smaller scales any more than for $\sigma_8 = 0.8$, because the 1-halo term still dominates several orders of magnitude at most.

The effect is notable however, on the linear power spectrum and therefore also the 2-halo term. Figure 5.7 clearly shows the free-streaming dampening for $\Omega_\nu = 0.03, 0.05$ and 0.1, with $\sigma_8 = 0.8$ as before. Note that the graphs do not completely coincide on the largest scales, this is due to inaccuracies during the normalization of $P^{\mathrm{lin}}_{\mathrm{dm}}(k)$ with and without correction for neutrinos.

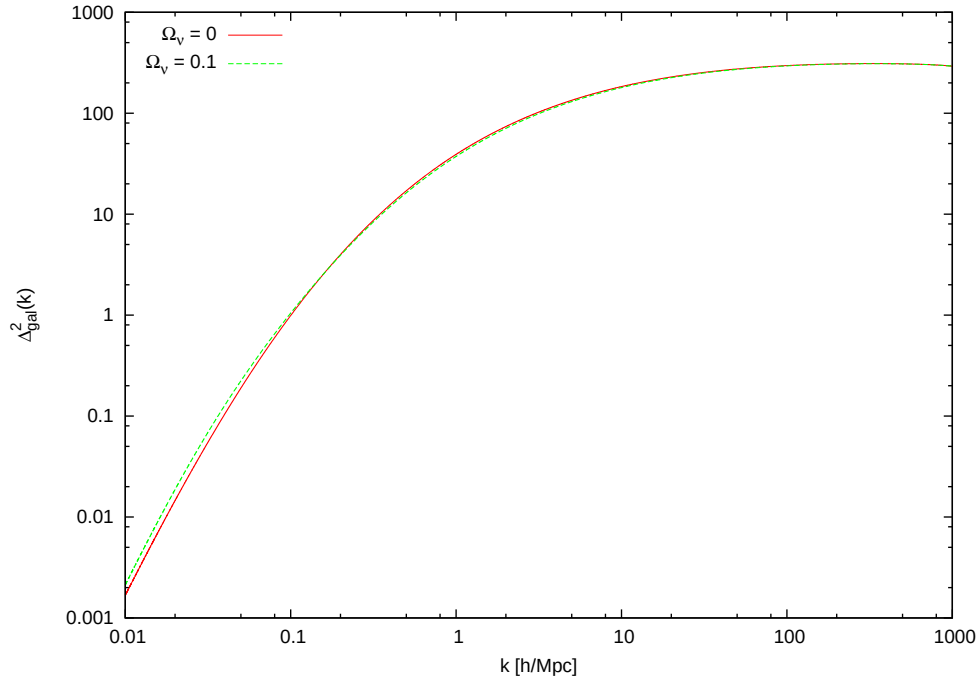

Figure 5.5: The galaxy power spectrum does at first glance not show any particular damping by massive neutrinos in this version of the model, due to the dominance of the 1-halo term on scales of interest. Even for a large neutrino mass (here is shown for $\Omega_\nu = 0.1$ for example) the 1-halo term is still dominates the 2-halo term many orders of magnitude, making it dominate the total power. The effect needs to be examined in a bit more detail to draw any conclusions. (Note: on the largest scales the model is inaccurate; in reality the curves should overlap towards $k \to 0$.)

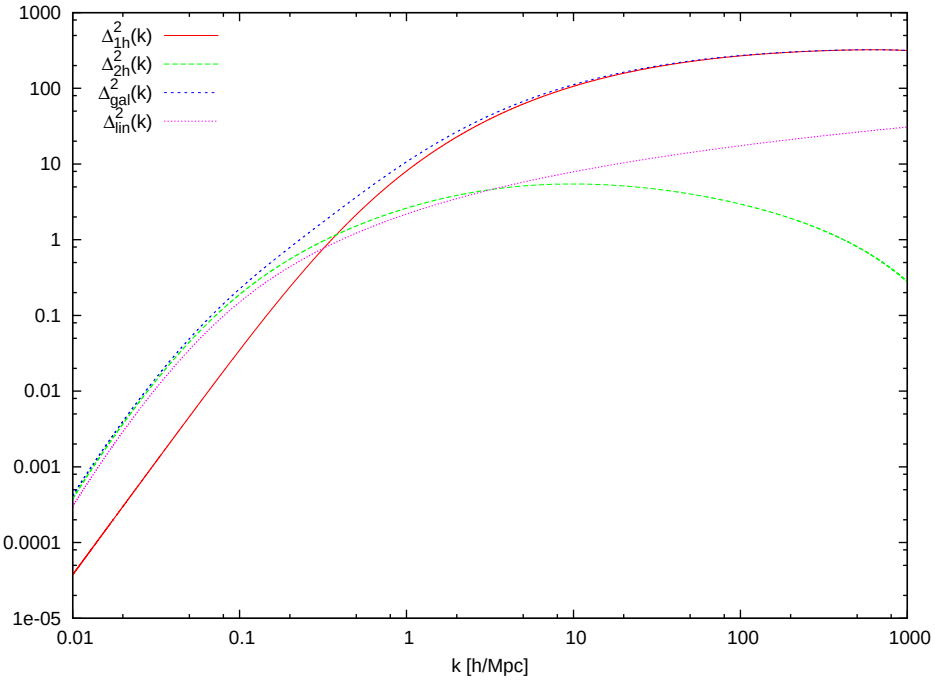

Figure 5.6: The galaxy power spectrum, plotted for $\sigma_8 = 0.6$, a visually better portrayal of the clear distinction between the 1-halo and 2-halo term making up the total power. The linear power spectrum is shown for reference.

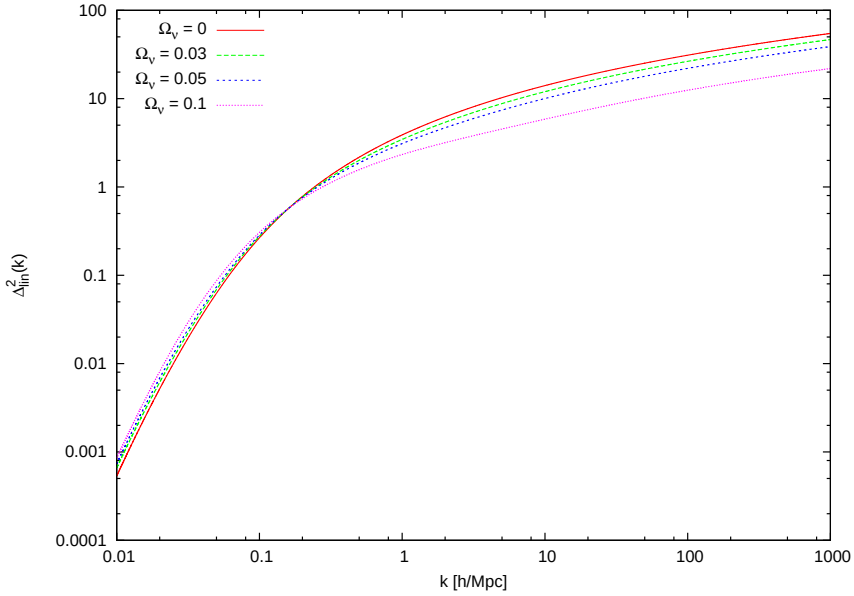

(a) Free-streaming suppression of linear power spectrum

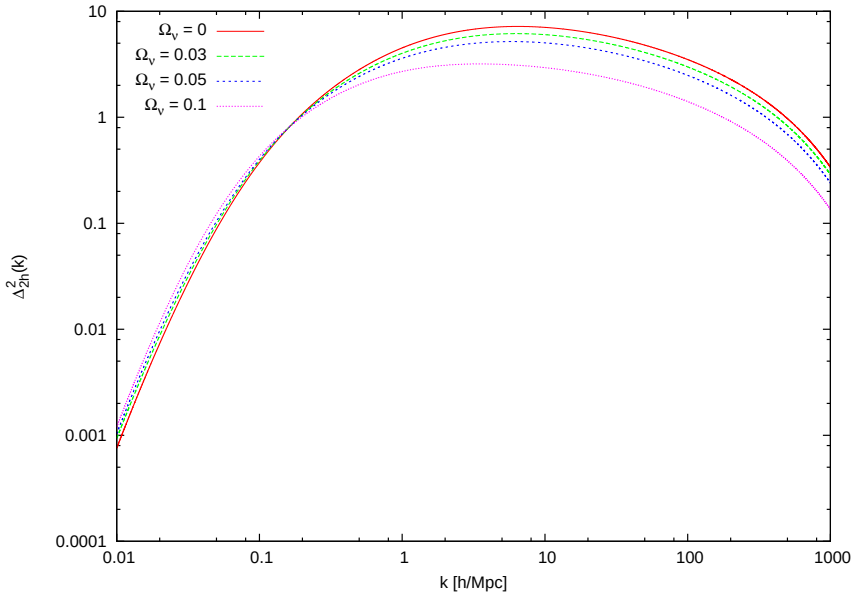

(b) Free-streaming suppression of 2-halo term

Figure 5.7: The inclusion of the modification (4.17) in the transfer function (4.14) due to massive neutrinos creates a suppression on the linear power spectrum and hence the 2-halo term towards smaller scales. Here $\Delta^2_{\rm lin}(k)$ and $\Delta^2_{\rm 2h}(k)$ is shown for three different values of the total neutrino mass, as well as the case $\Omega_\nu = 0$.

In order to draw any interesting conclusions about the effect of massive neutrinos, a reasonable approach is to measure the relative differences between the two cases. In Figure 5.8 is plotted the relative difference $(P_{\text{gal},\nu}(k) - P_{\text{gal}}(k))/P_{\text{gal}}(k)$, between the galaxy power spectrums with and without neutrino mass. The mentioned inaccuracies on large scales

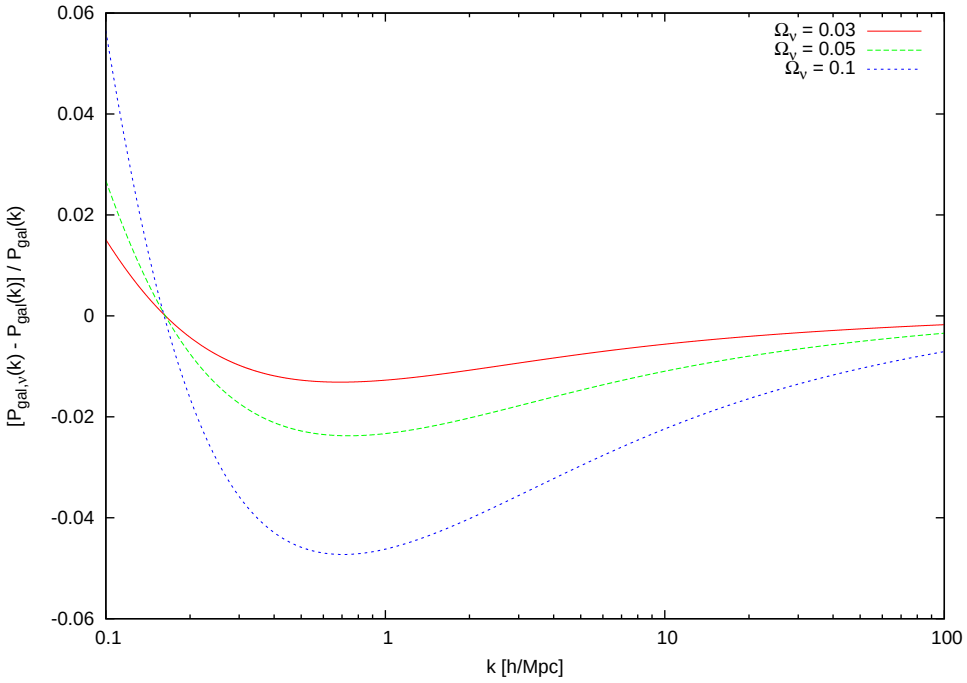

Figure 5.8: The relative difference on the total power spectrum due to massive neutrinos. The scales of interest are in the vicinity of $k \sim 1$ in this figure.

will propagate towards the smaller ones. When deciding on the largest relative difference to consider, and even though neutrino dampening in reality is expected to be noticable when scales become nonlinear (around $k = 0.1$), then because of the error on large csales it is necessary to put a limit for the minimum value of k which is meaningful for the plots. If we set this value to $k = 1$, then from the data making up the figure we can conclude on maximum relative differences of 0.0127, 0.0233, and 0.0462 for $\Omega_\nu = 0.03$, $\Omega_\nu = 0.05$ and $\Omega_\nu = 0.1$, respectively.

Having established that the previous plots of the galaxy power spectrum show a small, albeit measurable difference due to massive neutrinos, an alternative approach is next applied by also choosing the r.m.s. variance $\sigma(M)$ to depend on Ω_ν. This is theoretically a more plausible way of modelling, since the variance is that of the linear power spectrum, through which the neutrino mass damping will contribute. A rough power-law fit on $\sigma(M)$ is obtained directly from the linear power spectrum with the neutrino tweak (4.17) added:

$$\sigma(R) = \sigma_8 \left(\frac{R}{8h^{-1}\,\text{Mpc}} \right)^{-0.58}, \tag{5.2}$$

with $R = (3M/4\pi\bar{\rho})^{1/3}$. This expression is valid for $\Omega_\nu = 0.05$ and $\sigma_8 = 0.8$. A contribution from massive neutrinos on the mass variance would theoretically mean that both the 1-halo and 2-halo term will be affected. The new effect would come through the mass function as well as the halo bias function, since both depend on σ. Figure 5.9 shows the new form of $\sigma(M)$ together with the one without massive neutrinos, the mass function, and the halo bias function with this new form of $\sigma(M)$ incorporated, compared to the ones with $\Omega_\nu = 0$. When plotting the asscociated power spectra with this new modification, a problem occurs that unfortunately leads to the conclusion that the modified model cannot be pursued any further. The result of integrating the combined mass and halo bias function now somehow causes a reverse effect. This seems highly counter-intuitive considering the mass function has lower values over the mass range in total, and the increase in halo bias for high mass is not significant compared to the drop in mass function. For reference, the peculiar effect is shown in Figure 5.10.

There are numerous ways in which the halo model could be modified to further study and get more accurate predictions for the effect of massive neutrinos in the power spectrum. Some of these are mentioned in the next chapter. Nevertheless, having found the fractional difference values depicted in Figure 5.8, a conclusion from this can be obtained.

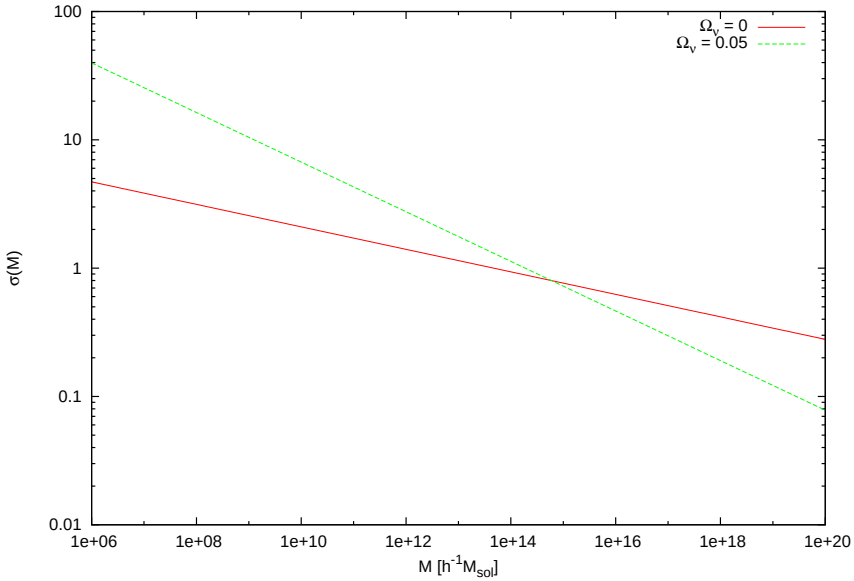

(a) The new form of $\sigma(M)$ dependent on neutrino mass shows the tilting effect compared to the case of no neutrinos. The form is valid for $\sigma_8 = 0.8$ and $\Omega_\nu = 0.05$.

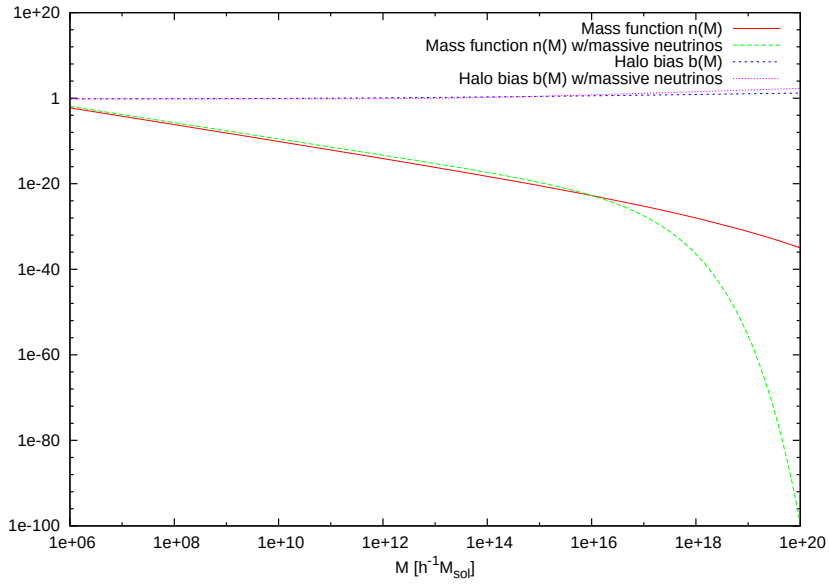

(b) The altered form of the mass function and halo bias function, for $\sigma_8 = 0.8$ and $\Omega_\nu = 0.05$. The bias is stronger for large mass halos when free-streaming occurs. The mass function falls steeply towards zero around $M = 10^{16} h^{-1} M_\odot$, which indicates vanishing density of mass perturbations above this value.

Figure 5.9: $\sigma(M)$ modified for massive neutrinos, together with mass and bias function

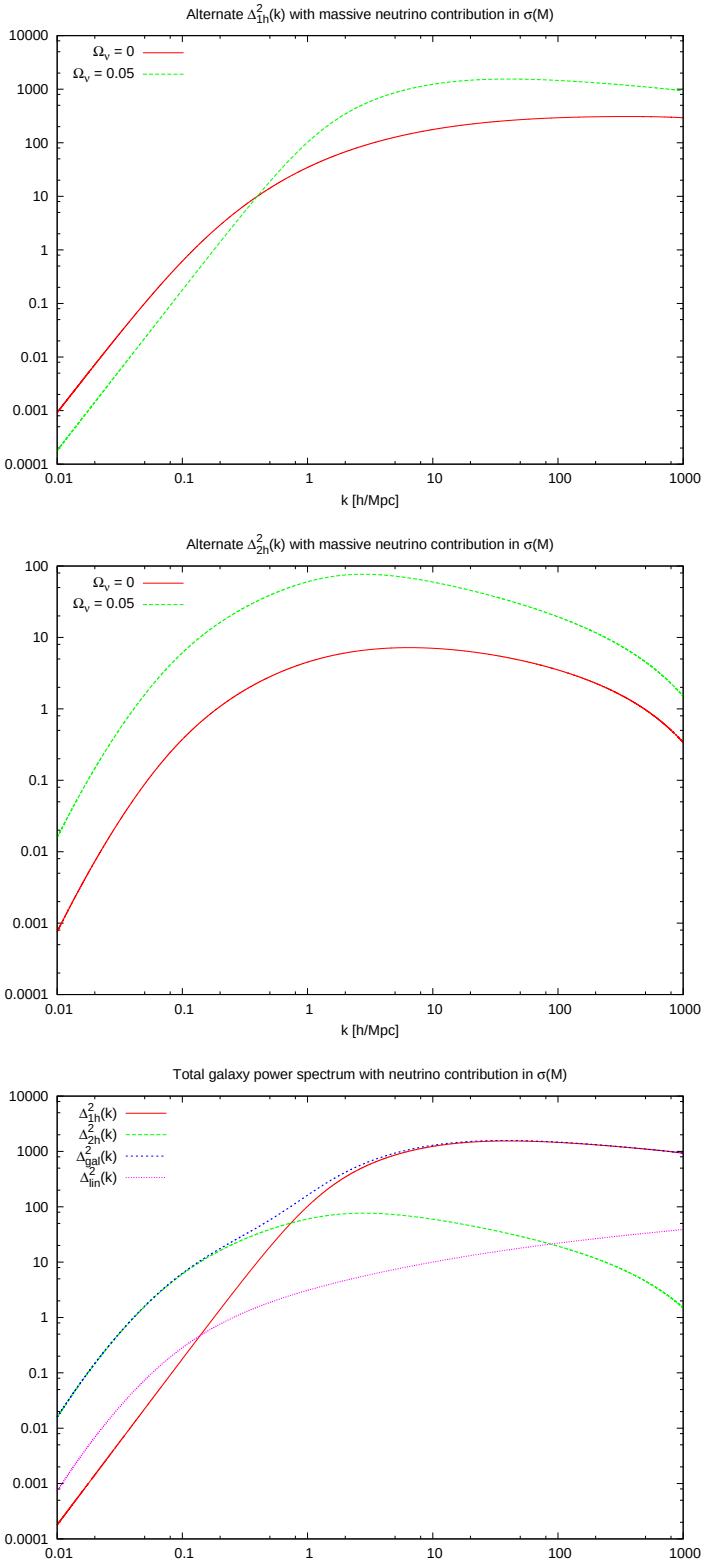

Figure 5.10: Letting the r.m.s. linear variance depend on Ω_ν through the fudge (5.2), creates effects on the power spectrum that is exactly the opposite of the effect massive neutrinos should cause. Since it proves difficult to see exactly what causes this flaw, the modified version of the halo model cannot be pursued. Note that the linear power spectrum, which is the same as before, does not agree with the 2-halo term as it should on large scales.

Chapter 6

Conclusion

> The world always seems brighter when you've just made something that wasn't there before.
>
> —Neil Gaiman

6.1 Summary

The goal of this thesis was to study how the power spectrum of the galaxy distribution could be modeled through the halo model, a simple model of non-linear structure formation. The simplicity of the halo model lies in the assumption that all mass is confined to virialized halos of different sizes and mass. The power spectrum can be looked at as the sum of two terms: One on the quasi-linear scale between two halos, characterized by a halo occupation distribution, and one for the non-linear regime within single halos, determined by a halo density profile. Taking a phenomenological approach, a lot of the functions and parameters comprising the power spectrum was taken from empirical studies, as well as using simple analytical expressions for other parts.

Using the halo model, the effect of adding massive neutrinos into the picture was studied. The neutrinos were allowed to affect the linear power spectrum only, such that the inter-halo term of the galaxy power spectrum in turn was modified. Massive neutrinos are expected to cause a smoothing out of the power on small scales due to free-streaming, which in turn means a suppression of the power spectrum. Relative differences between the galaxy power spectra including and not including massive neutrinos on a scale $k = 1h/\text{Mpc}$ was found to be 1.27%, 2.33% and 4.62% for $\Omega_\nu = 0.03, 0.05$ and 0.1, respectively.

6.2 Conclusion

The question that remains from the results above is whether or not this can be thought of as an interesting effect; an effect above 4–5% would be a desired result. However, the observed galaxy power spectrum contains less noise when looking at small scales. A

suppression of about 1–2% should therefore be taken into consideration as a marginally interesting effect, especially towards future observations. Another feature to look at is how using the nonlinear halo model for looking at neutrino suppression compares to the linear case. A comparison to the analysis of the linear power spectrum shown in Figure 5.7 depicts a much larger suppression for this model than in the galaxy spectrum in Figure 5.5; examining the data for $k = 1h/\text{Mpc}$ reveals a dampening effect of order 10 times the values for the nonlinear case. In relation to the linear power spectrum, the halo model does therefore not enhance the effect of massive neutrinos when constructed the way chosen for this project.

There are many ways in which this model can be constructed differently, as mentioned in Section 1.2.1. A few examples of things that were not considered in this thesis include:

- **A more detailed and accurate modelling of the r.m.s. variance of the linear power spectrum.** As an example, the article by Ma [22] considers a general form of $\sigma(M)$ which can be used for both the case with massive neutrinos and for $\Omega_\nu = 0$, directly based on the linear spectrum with transfer function (4.14) with the modification (4.17).

- **Implementing a different density profile.** There is no particular reason why the NFW form is better than others; for example, in numerical simulations both the NFW and M99 [15] profile provides very good descriptions of the density run around the center of virialized halos. The profiles differ on scales smaller than the scale radius r_s, and whichever of the two is better is still debated.

- **Mass-dependent concentration parameter.** As mentioned in Chapter 4, there is a slight decrease in the concentration parameter with increasing mass, and the power law form could easily be implemented. The mean value found by Collister & Lahav were used for the modelling for the reason that many other empirical results were taken from this article, where the mass dependence on the concentration parameter was considered a subtlety and therefore ignored.

- **Studying higher order correlations.** A feature that has not been mentioned at all during the course of this project is that higher order correlation functions can be taken into account. The Fourier transforms of the three- and four-point correlation functions are called the bispectrum and trispectrum, respectively. Using such higher order statistics, the model will feature 3-halo and 4-halo terms, and it will give more detailed information in the form of a more complete statistical description of the clustering (The information gathered from the power spectrum is equivalent to the variance of a random variable only). A description of higher-order correlations requires the use of higher-order perturbation theory; a discussion of this can be found in [7].

- **Aspherical collapse.** The shape of what are to become halos is in reality seldom spherical, and neither is the form of the collapse. If halos are intitially aspherical,

tidal interactions between neighboring density fluctuations create nonradial motions which oppose collapse. This means that virialized clumps form later than in the spherical collapse model. A discussion of an ellipsoidal collapse model is discussed in [24]. The goal of this thesis mainly considered studying relative shapes of the power spectra however, while correcting for aspherical collapse would play a part in improving the halo model as a tool for comparison with observations.

As for the ongoing quest to constrain the mass of the neutrino, the five-year data gathered from WMAP recently released is still on the preliminary stage, with an upper limit of 1.3 eV at 2σ-level for the total mass. This needs to be coordinated with results from other experiments, and the incorporating of current results from studies of large-scale structure is expected to favour a mass scale towards the sub-eV range.

Appendix A

Mathematical expressions

In this appendix we gather for convenience some important functions and expressions used in the introductional chapters of this thesis.

A.1 Special functions

The Error Function

Definition:

$$\mathrm{erf}(x) \equiv \frac{2}{\sqrt{\pi}} \int_0^x e^{-t^2} \mathrm{d}t \tag{A.1}$$

Derivative:

$$\frac{\mathrm{d}}{\mathrm{d}x}\mathrm{erf}(x) = \frac{2}{\sqrt{\pi}} e^{-x^2} \tag{A.2}$$

The Gamma Function

Definitions:

$$\begin{aligned} \Gamma(x) &\equiv \int_0^\infty t^{x-1} e^{-t} \mathrm{d}t \\ \Gamma(x+1) &= x\Gamma(x) \end{aligned}$$

Properties:

$$\begin{aligned} \Gamma(1) = 1, \quad \Gamma\left(\frac{1}{2}\right) &= \sqrt{\pi} \\ \Gamma(n+1) = n\Gamma(n) = \ldots = n!\Gamma(1) &= n! \qquad \forall n \in \mathbb{N} \end{aligned} \tag{A.3}$$

Series representation of $\sin x$ and $\cos x$

$$\sin x = x - \frac{x^3}{3!} + \frac{x^5}{5!} - \ldots = \sum_{n=0}^{\infty} (-1)^n \frac{x^{2n+1}}{(2n+1)!} \tag{A.4}$$

$$\cos x = 1 - \frac{x^2}{2!} + \frac{x^4}{4!} - \ldots = \sum_{n=0}^{\infty} (-1)^n \frac{x^{2n}}{(2n)!} \tag{A.5}$$

Sine and cosine integrals

Definitions:

$$\mathrm{Si}(x) = \int_0^x \frac{\sin t}{t} \mathrm{d}t \tag{A.6}$$

$$\begin{aligned} \mathrm{Ci}(x) &= -\int_x^{\infty} \frac{\cos t}{t} \mathrm{d}t \\ &= \gamma + \ln x + \int_0^x \frac{\cos t - 1}{t} \mathrm{d}t, \end{aligned} \tag{A.7}$$

where $\gamma = 0.5772156649\ldots$ is Euler's constant.

A.2 Some integrals

If a, k are positive integers and C is an integration constant, then

$$\int e^{-ax^2} \mathrm{d}x = \frac{1}{2}\sqrt{\frac{\pi}{a}} \mathrm{erf}(\sqrt{a}x) + C \tag{A.8}$$

$$\int_{-\infty}^{\infty} x^k e^{-ax^2} \mathrm{d}x = 2\int_0^{\infty} x^k e^{-ax^2} \mathrm{d}x = a^{-\frac{k+1}{2}} \Gamma\left(\frac{k+1}{2}\right) \tag{A.9}$$

where the error and gamma functions are defined above.

Appendix B

Program Code

B.1 Notes

The following appendix displays the program code for this thesis written in the FORTRAN 90 language. Comments are provided throughout to make the code as comprehensible as possible. There are however, a couple of points which need to be considered beforehand.

In order to perform the integration of functions, the method of Gauss-Legendre quadrature has been chosen. Gaussian quadrature in general is an method which seeks to obtain the best numerical estimate of an integral by systematically picking the optimal abscissas, or evaluation points, at which to evaluate a function $f(x)$. The n-point approximation is generally written on the form

$$I = \int_{-1}^{1} f(x)\mathrm{d}x \approx \sum_{i=1}^{n} w_i f(x_i), \tag{B.1}$$

where w_i are the weights corresponding to each abcissa x_i. In Legendre quadrature, these evaluation points are the i^{th} roots of the Legendre polynomials $P_n(x)$, a class of orthogonal polynomials which are the solutions to the Legendre differential equation. They can be expressed through Rodrigues' formula:

$$P_n(x) = \frac{1}{2^n n!}\frac{\mathrm{d}^n}{\mathrm{d}x^n}\left[(x^2+1)^n\right]. \tag{B.2}$$

The weights are given by

$$w_i = \frac{2}{(1-x_i^2)(P_n'(x_i))^2}. \tag{B.3}$$

A general integral over an interval $[a,b]$ must be changed into an interval over $[-1,1]$ in order for Gaussian quadrature to apply. We then have

$$\begin{aligned} \int_a^b f(x)\mathrm{d}x &= \frac{b-a}{2}\int_{-1}^{1} f\left(\frac{b-a}{2}x + \frac{a+b}{2}\right)\mathrm{d}x, \qquad \text{which gives} \\ I &\approx \frac{b-a}{2}\sum_{i=1}^{n} w_i f\left(\frac{b-a}{2}x_i + \frac{a+b}{2}\right). \end{aligned} \tag{B.4}$$

There exist several numerical libraries with packages devoted to integration techniques. The method in this thesis is chosen from *Numerical Recipes in Fortran* (see [20]), and is manifested below through the call to the routine `gauleg`.[1]

Another routine taken from [20] is the one evaluating the sine and cosine integrals. The routine, called `cisi`, takes the argument and returns the values for the cosine and sine integral evaluated in that argument, according to the series representation described in Appendix A.

The text file `params.txt`, together with a routine for reading values from this file into the program provides the freedom from having to compile the code every time we change parameters such as Ω_ν or the integration and function evaluation intervals.

[1] There are of course many freely available codes to choose from as well, such as the GNU Scientific Library [25].

B.2 F90 code

Listing B.1: halopower.f90

```
1  PROGRAM halomodel
2
3    !!!!!!!!!!!!!!!!!!!!!!!!!!!!!!!!!!!!!!!!!!!!!!!!!!!!!!!!!!!!!!!!!!!!!!!
4    !!!!!!!!!!!!!!!!!!!!!!!!!!!!!!!!!!!!!!!!!!!!!!!!!!!!!!!!!!!!!!!!!!!!!!!
5    !! A simple model for modeling the galaxy power spectrum. !!
6    !!!!!!!!!!!!!!!!!!!!!!!!!!!!!!!!!!!!!!!!!!!!!!!!!!!!!!!!!!!!!!!!!!!!!!!
7    !!!!!!!!!!!!!!!!!!!!!!!!!!!!!!!!!!!!!!!!!!!!!!!!!!!!!!!!!!!!!!!!!!!!!!!
8    !!
9    !! INPUT: value of omega_nu, alternatively sigma8, the
10   !! number of points in which to perform gaussian quadrature
11   !! and the minimum and maximum values of mass and scale.
12   !! This input is through a text file called params.txt, an
13   !! example of which is shown at the end of this chapter.
14   !!
15   !! OUTPUT: several .dat files containing plottable functions
16   !! including
17   !! * The total galaxy power spectrum
18   !! * The 1-halo and 2-halo terms
19   !! * The linear power spectrum
20   !! * The components of the integrands of the 1-halo and
21   !!   2-halo terms: mass variance, mass function, halo bias,
22   !!   mean halo occupation number, NFW density profile
23   !!   (depends on both m and k, so beware that the file becomes
24   !!   HUGE if the functions are evaluated for many points in
25   !!   mass and scale!).
26   !! * Relative difference between galaxy power spectra with and
27   !!   without massive neutrinos.
28   USE nrtype
29   USE funcparams
30   IMPLICIT NONE
31
32   INTEGER :: i,j,nm,nk
33   REAL(dp) :: min_m, max_m, min_k, max_k
34   REAL(dp) :: ki,mj,dmj
35   REAL(dp) :: lower, upper
36   REAL(dp) :: int1h,int2h
37   REAL(dp) :: sum1h,sum2h
38   REAL(dp),DIMENSION(:),ALLOCATABLE :: m, wm, k, wk
39
40   ! 'Delta' signifies dimensionless power spectrum
41   REAL(dp) :: p1h,p2h,p2h_nu,pgal,pgal_nu
42   REAL(dp) :: deltap1h,deltap2h,deltapgal,deltaplin
43   REAL(dp) :: deltap2h_nu,deltapgal_nu,deltaplin_nu
44   REAL(dp) :: rel_pgal
45
46   CHARACTER(LEN=128) :: params
47
```

```
48    ! Read the parameter file and get input data:
49    params = 'params.txt'
50    CALL read_params(params,nk,nm,min_m,max_m,min_k,max_k)
51
52    ! Arrays for evaluating the Gauss-Legendre abcissas
53    ! and weights in mass and scale (note that wk is needed
54    ! as input by the routine, but not in the program).
55    ALLOCATE(m(1:nm))
56    ALLOCATE(wm(1:nm))
57    ALLOCATE(k(1:nk))
58    ALLOCATE(wk(1:nk))
59
60    !open data files for writing
61    OPEN(UNIT=100, FILE='hodmoment.dat', FORM='FORMATTED', ACTION='READWRITE')
62    OPEN(UNIT=101, FILE='massfunc.dat', FORM='FORMATTED', ACTION='READWRITE')
63    OPEN(UNIT=102, FILE='biasfunc.dat', FORM='FORMATTED', ACTION='READWRITE')
64    OPEN(UNIT=103, FILE='ugal.dat', FORM='FORMATTED', ACTION='READWRITE')
65    OPEN(UNIT=104, FILE='p1h.dat', FORM='FORMATTED', ACTION='READWRITE')
66    OPEN(UNIT=105, FILE='plin.dat', FORM='FORMATTED', ACTION='READWRITE')
67    OPEN(UNIT=106, FILE='p2h.dat', FORM='FORMATTED', ACTION='READWRITE')
68    OPEN(UNIT=107, FILE='pgal.dat', FORM='FORMATTED', ACTION='READWRITE')
69    OPEN(UNIT=555, FILE='sigma.dat',FORM='FORMATTED', ACTION='READWRITE')
70    OPEN(unit=666, FILE='relatives.dat', FORM='FORMATTED',ACTION='READWRITE')
71
72    !Calculate the abcissas and weights for evaluating
73    !the integrals over mass. Note that we evaluate through
74    !logarithmic values because the scales in mass are over
75    !several orders of magnitude, this way we ensure that enough
76    !points are calculated for the smalles masses.
77    lower = LOG10(min_M)
78    upper = LOG10(max_M)
79    wm    = 0.0_dp
80    CALL gauleg(lower,upper,m,wm,nm)
81
82    !We do the same for scale k even if we do not integrate;
83    !the method ensures reasonable points are chosen for the
84    !scales on which we evaluate the power spectra,
85    lower = log10(min_k)
86    upper = log10(max_k)
87    wk    = 0.0_dp
88    CALL gauleg(lower,upper,k,wk,nk)
89
90
91    PRINT '(/,"This␣may␣take␣a␣minute␣or␣two,␣depending␣on␣choice␣of␣nk␣and␣nm
          .␣Enjoy␣your␣coffee!",/)'
92
93    ! Compute normalization constants for the (hot+) cold dark matter
94    ! power spectrum. Write to screen.
95    CALL normalize_pdmlin(omega_m,omega_nu,h,sigma8,nk,min_k,max_k)
96    PRINT '(/,"Normalization␣constant␣for␣sigma8␣=␣",f4.2,"␣is␣",f10.2,".")',
          sigma8,norm
```

```
97    PRINT '(/,"Normalization␣constant␣for␣sigma8␣=␣",f4.2,"␣with␣massive␣
          neutrinos␣is␣",f10.2,".")',sigma8,normnu
98
99    ! For each value of k there is an integral over mass:
100   DO i = 1,nk
101      ki = 10.0_dp**k(i) ! remove logarithm
102
103      sum1h    = 0.0_dp
104      sum2h    = 0.0_dp
105
106      ! a test to write out how far we are in the process
107      IF (INT(100*i/nk) .EQ. INT(1+(100*(i-1)/nk))) THEN
108         PRINT '(2x,"Processing␣k␣values...␣",i3,"%␣complete.")',INT(100*(i
               -1)/nk)
109      END IF
110      IF(i.EQ.nk) THEN
111         PRINT '(2x,"Almost␣done...")'
112      END IF
113
114      ! Start the integration over mass
115      DO j = 1,nm
116         mj = 10.0_dp**m(j) ! get rid of logarithm
117         dmj = wm(j)
118
119         CALL compute_1h_integrand(ki,mj,Omega_m,sigma8,h,int1h)
120         CALL compute_2h_integrand(ki,mj,Omega_m,sigma8,h,int2h)
121
122         ! The factors m*ln(10) are to compensate for the fact
123         ! that the abcissas were computed as logarithmic values
124         ! when multiplying the weights.
125         sum1h    = sum1h + int1h * dmj * LOG(10.0_dp) * mj
126         sum2h    = sum2h + int2h * dmj * LOG(10.0_dp) * mj
127
128         !Write to files...
129         IF(ki.EQ.10**k(1)) THEN
130            !functions depending on m only need only be written for one
131            !k loop; the mass values are the same for each one.
132            WRITE(UNIT=555,FMT="(2(es15.8,2x))"),mj,sigma
133            WRITE(UNIT=100,FMT="(2(es15.8,2x))"),mj,hodmoment
134            WRITE(UNIT=101,FMT="(2(es15.8,2x))"),mj,massfun
135            WRITE(UNIT=102,FMT="(2(es15.8,2x))"),mj,biasfun
136         endif
137
138         WRITE(UNIT=103,FMT="(3(es15.8,2x))"),ki,mj,ugal
139
140      END DO !End loop over mass
141
142      !Calculate 1-halo term and write to file
143      p1h          = sum1h
144      deltap1h     = (ki*ki*ki*p1h)/(2._dp*PI_D*PI_D)
145      WRITE(UNIT=104,FMT="(2(es15.8,2x))"),ki,deltap1h
```

```
146
147         !Calculate linear dark matter power spectrum and write to file
148         CALL compute_pdmlin(ki,omega_m,omega_nu,h,sigma8,nk,min_k,max_k)
149         deltaplin     = (ki*ki*ki*pdmlin)/(2._dp*PI_D*PI_D)
150         deltaplin_nu  = (ki*ki*ki*pdmlin_nu)/(2._dp*PI_D*PI_D)
151         WRITE(UNIT=105,FMT="(3(es15.8,2x))"),ki,deltaplin,deltaplin_nu
152
153         !Calculate 2-halo term and write to file
154         p2h           = pdmlin*sum2h*sum2h
155         p2h_nu        =  pdmlin_nu*sum2h*sum2h
156         deltap2h      = (ki*ki*ki*p2h)/(2._dp*PI_D*PI_D)
157         deltap2h_nu   = (ki*ki*ki*p2h_nu)/(2._dp*PI_D*PI_D)
158         WRITE(UNIT=106,FMT="(3(es15.8,2x))"),ki,deltap2h,deltap2h_nu
159
160         !Calculate the total galaxy power spectrum and write to file
161         pgal          = p1h+p2h
162         pgal_nu       = p1h+p2h_nu
163         deltapgal     = (ki*ki*ki*pgal)/(2._dp*PI_D*PI_D)
164         deltapgal_nu  = (ki*ki*ki*pgal_nu)/(2._dp*PI_D*PI_D)
165         WRITE(UNIT=107,FMT="(3(es15.8,2x))"),ki,deltapgal,deltapgal_nu
166
167         !Calculate relative difference in the two cases of power spectra
168         !and write to file
169         rel_pgal= (pgal_nu-pgal)/pgal
170         WRITE(UNIT=666,FMT="(2(es15.8,2x))"),ki,rel_pgal
171
172     END DO !end loop over scale k
173
174     DEALLOCATE(wm)
175     DEALLOCATE(m)
176     DEALLOCATE(wk)
177     DEALLOCATE(k)
178
179     CLOSE(UNIT=100)
180     CLOSE(UNIT=101)
181     CLOSE(UNIT=102)
182     CLOSE(UNIT=103)
183     CLOSE(UNIT=104)
184     CLOSE(UNIT=105)
185     CLOSE(UNIT=106)
186     CLOSE(UNIT=107)
187     CLOSE(UNIT=555)
188     close(unit=666)
189
190 END PROGRAM halomodel
```

Listing B.2: utils.f90

```
1  MODULE funcparams
2
3     ! A module containing subroutines, functions and parameters for use
4     ! in halopower.f90. Note: all variables ending in 'nu' means it has
5     ! to do with an added contribution from massive neutrinos (allthough
6     ! the variable 'nu' alone is the mass variable depending on the variance).
7
8     USE nrtype
9     IMPLICIT NONE
10
11    !constants related to cosmology which are read from params.txt
12
13    REAL(dp)   :: omega_nu, sigma8
14
15    ! these are variables in which the function values calculated are stored:
16    !
17    ! massfun     = the mass function
18    ! sigma       = the mass variance of linear power spectrum
19    ! biasfun     = halo bias function
20    ! ugal        = NFW form of the normalized, Fourier transformed
21    !               density profile
22    !               of the halo distribution
23    ! hodmoment   = the mean halo occupation number, 1st moment of the HOD
24    ! pdmlin      = linear power spectrum, with ('_nu') or without massive
25    !                neutrinos
26    ! norm        = normalization constant for the corresponding linear
27    !               spectrum above
28
29    REAL(dp)   ::  massfun,sigma,biasfun
30    REAL(dp)   ::  ugal,hodmoment
31    REAL(dp)   ::  pdmlin, pdmlin_nu, norm, normnu
32
33    ! Model specific parameter values that are not changed:
34    ! omega_m     = Density parameter of matter (cdm + hdm)
35    ! h           = Dimensionless Hubble constant
36    ! rhobar      = Mean density of a spacially flat universe
37    ! Delta_vir   = Overdensity of halo at virialization
38    ! conc_param = Mean concentration parameter (Collister/Lahav)
39    ! p,q,Astar   = Numerically fitted constants for the mass function
40    !               (Collister/Lahav)
41    ! ngal        = mean number density of galaxy distribution
42    !               (Collister/Lahav)
43    REAL(dp),PARAMETER :: omega_m    = 0.3_dp
44    REAL(dp),PARAMETER :: h          = 0.7_dp
45    REAL(dp),PARAMETER :: rhobar     = 2.775e11_dp ! units h^2 Msol Mpc^-3
46    REAL(dp),PARAMETER :: Delta_vir  = 200.0_dp
47    REAL(dp),PARAMETER :: conc_param = 2.4_dp
48    REAL(dp),PARAMETER :: delta_c    = 1.686_dp
49    REAL(dp),PARAMETER :: p          = 0.3_dp
50    REAL(dp),PARAMETER :: q          = 0.707_dp
```

```
51    REAL(dp),PARAMETER :: Astar      = 0.3222_dp
52    REAL(dp),PARAMETER :: ngal       = 0.00506_dp  ! units h^3 Mpc^-3
53
54
55  CONTAINS
56
57    SUBROUTINE compute_1h_integrand(k,m,om,s8,h,int1h)
58
59      ! Computes the integrand in the 1-halo term of the galaxy power spectrum
60      IMPLICIT NONE
61
62      REAL(dp),INTENT(in) :: k,m,om,s8,h
63      REAL(dp)            :: int1h
64
65      ! These give the values of variables massfunc,hodmoment and ugal,
66      ! respectively
67      CALL compute_mass_function(m,om,s8,h)
68      CALL compute_hod_expectval(m)
69      CALL compute_ugal(k,m,conc_param)
70
71      int1h   = massfun*hodmoment*hodmoment*ugal*ugal/(ngal*ngal)
72
73    END SUBROUTINE compute_1h_integrand
74
75    SUBROUTINE compute_2h_integrand(k,m,om,s8,h,int2h)
76
77      ! Computes the integrand in the 2-halo term of the galaxy power spectrum
78      IMPLICIT NONE
79
80      REAL(dp),INTENT(in) :: k,m,om,s8,h
81      REAL(dp)            :: int2h
82
83      ! These give the values of variables massfunc,biasfunc,hodmoment
84      ! and ugal, respectively.
85      CALL compute_mass_function(m,om,s8,h)
86      CALL compute_bias_function(m,om,s8,h)
87      CALL compute_hod_expectval(m)
88      CALL compute_ugal(k,m,conc_param)
89
90      int2h   = massfun*biasfun*hodmoment*ugal/ngal
91
92    END SUBROUTINE compute_2h_integrand
93
94  !!!!!!!!!!!!!!!!!!!!!!!!!!!!!!!!!!!!!!!!!!!!!!!!!!!!!!!!!!!!!!!!!!!!!!!!
95  !! ROUTINES TO COMPUTE THE VARIABLES USED IN THE ABOVE NOW FOLLOWS !!
96  !!!!!!!!!!!!!!!!!!!!!!!!!!!!!!!!!!!!!!!!!!!!!!!!!!!!!!!!!!!!!!!!!!!!!!!!
97
98    SUBROUTINE compute_mass_function(m,om,s8,h)
99      IMPLICIT NONE
100
101     REAL(dp), INTENT(in) :: m,om,s8,h
```

```
102       REAL(dp)                  :: fact,gamma,nu
103
104       CALL compute_sigma(m,om,s8,h)
105       nu = (delta_c*delta_c) / (sigma*sigma)
106       gamma     = om*h
107       fact      = 0.3_dp*gamma+0.2_dp
108       nu        = (delta_c*delta_c) / (sigma*sigma)
109
110       massfun = (2._dp*fact/3._dp)*(rhobar/(m*m))*nufnu(nu)
111
112     CONTAINS
113
114       FUNCTION nufnu(x)
115         IMPLICIT NONE
116         REAL(dp), INTENT(in) :: x
117         REAL(dp)             :: Astar,nufnu,qnu
118
119         qnu   = q*x
120         Astar = 0.3222_dp
121         nufnu =  Astar * (1._dp+qnu**(-p)) * &
122              sqrt(qnu/(2._dp*PI_D)) * exp(-qnu/2._dp)
123       END FUNCTION nufnu
124
125     END SUBROUTINE compute_mass_function
126
127   !!!!!!!!!!!!!!!
128
129     SUBROUTINE compute_bias_function(m,om,s8,h)
130       IMPLICIT NONE
131
132       REAL(dp), INTENT(in) :: m,om,s8,h
133       REAL(dp)             :: nu,qnu
134
135       CALL compute_sigma(m,om,s8,h)
136
137       nu    = (delta_c*delta_c) / (sigma*sigma)
138       qnu   = q*nu
139
140       biasfun = 1._dp + ( (qnu-1._dp) / delta_c ) + &
141            ( (2._dp*p/delta_c) / (1._dp+qnu**p) )
142
143     END SUBROUTINE compute_bias_function
144
145   !!!!!!!!!!!!!!!
146
147     SUBROUTINE compute_sigma(m,om,s8,h)
148       IMPLICIT NONE
149
150       REAL(dp),INTENT(in) :: m,om,s8,h
151       REAL(dp)            :: mstar,gamma,pot
152
```

```
153       gamma = om*h
154       pot   = (0.3_dp*gamma+0.2_dp)/3._dp
155       mstar = (4._dp*PI_D*rhobar*8._dp*8._dp*8._dp)/3._dp
156
157       sigma = s8*(mstar/m)**pot
158
159     END SUBROUTINE compute_sigma
160
161   !!!!!!!!!!!!!!!
162
163     SUBROUTINE compute_hod_expectval(m)
164       IMPLICIT NONE
165
166       REAL(dp), INTENT(in) :: m
167       REAL(dp)             :: beta, m0
168
169       beta = 0.99_dp
170       m0   = 10.0_dp**(13.5)
171
172       hodmoment = (m/m0)**beta
173
174     END SUBROUTINE compute_hod_expectval
175
176   !!!!!!!!!!!!!!!!
177
178     SUBROUTINE compute_ugal(k,m,c)
179       IMPLICIT NONE
180
181       REAL(dp), INTENT(in) :: k,m,c
182       REAL(dp)             :: scalerad,kappa
183       REAL(dp)             :: ci,si,cik,sik,cick,sick
184
185       scalerad = rs(m,c)
186       kappa    = k*scalerad
187
188       ! calculate sine and cosine integrals:
189       CALL cisi(kappa,ci,si)
190       cik  = ci
191       sik  = si
192       CALL cisi((kappa*(1+c)),ci,si)
193       cick = ci
194       sick = si
195
196       ugal = (1._dp/g(c))                    * &
197            (                                   &
198            SIN(kappa)*(sick-sik)             - &
199            SIN(c*kappa)/((1+c)*kappa)        + &
200            COS(kappa)*(cick-cik)               &
201            )
202
203     CONTAINS
```

```
204       FUNCTION rs(x,c)
205         IMPLICIT NONE
206
207         REAL(dp), INTENT(in) :: x,c
208         REAL(dp)             :: rs
209
210         rs = ((3._dp*x)/                          &
211               (4._dp*PI_D*Delta_vir*rhobar*c**3))&
212               **(1._dp/3._dp)
213       END FUNCTION rs
214
215       FUNCTION g(c)
216         REAL(dp), INTENT(in) :: c
217         REAL(dp)             :: g
218
219         g = LOG(1+c) - (c/(1._dp+c))
220       END FUNCTION g
221
222     END SUBROUTINE compute_ugal
223
224   !!!!!!!!!!!!!!!!!!!!!!!!!!!!!!!!!!!!!!!!!!!!!!!!!!!!!!!!!!!!!!!!!!!!!!
225   !! ROUTINES CONCERNING THE LINEAR DARK MATTER POWER SPECTRUM !!
226   !!!!!!!!!!!!!!!!!!!!!!!!!!!!!!!!!!!!!!!!!!!!!!!!!!!!!!!!!!!!!!!!!!!!!!
227
228     SUBROUTINE compute_pdmlin(k,om,onu,h,s8,n,min,max)
229
230       ! The dark matter power spectrum, computed for both the case of
231       ! massive neutrinos and without.
232       IMPLICIT NONE
233
234       INTEGER,  INTENT(in) :: n
235       REAL(dp), INTENT(in) :: k,om,onu,h,s8,min,max
236       REAL(dp)             :: power
237
238       ! Compute the cold dark matter power spectrum, add
239       ! massive neutrino fudge where necessary and multiply
240       ! with corresponding calculated normalization constant
241       ! (see below).
242       call compute_pcdmlin(k,om,h,power)
243       pdmlin    = power*norm
244       pdmlin_nu = power * powernu(k,onu,h)*normnu
245
246     CONTAINS
247
248       FUNCTION powernu(k,onu,h)
249         IMPLICIT NONE
250
251         REAL(dp), INTENT(in) :: k,onu,h
252         REAL(dp)             :: powernu,Gamma,x,pot
253         REAL(dp), PARAMETER  :: e1 = 0.004321_dp
254         REAL(dp), PARAMETER  :: e2 = 2.217e-6_dp
```

```
255         REAL(dp), PARAMETER   :: e3 = 11.63_dp
256         REAL(dp), PARAMETER   :: e4 = 3.317_dp
257
258         Gamma = onu*h
259         x     = k/Gamma
260         pot   = onu**(1.05_dp)
261
262         powernu = ((1._dp+e1*x**(0.5_dp*e4)+e2*x**e4) / &
263               (1._dp+e3*x**e4))**pot
264
265       END FUNCTION powernu
266
267     END SUBROUTINE compute_pdmlin
268
269   !!!!!!!!!!!!!!
270
271     SUBROUTINE normalize_pdmlin(om,onu,h,s8,n,min,max)
272
273       ! This routine integrates the dark matter power spectrum
274       ! over a chosen interval smoothed by a top-hat window on
275       ! the 8 h^{-1}Mpc scale and computes the normalization
276       ! constant for the spectrum by dividing the given squared
277       ! value of sigma8 by the answer.
278       IMPLICIT NONE
279
280       REAL(dp), INTENT(in)      :: om,onu,h,s8,min,max
281       INTEGER, INTENT(in)       :: n
282       INTEGER                   :: i
283       REAL(dp),DIMENSION(1:n)   :: kk, dkk
284       REAL(dp)                  :: integ,integnu,ocdm,power,plin,plin_nu
285       REAL(dp)                  :: kki,dkki,sum,sumnu,lower,upper
286
287       ocdm=om-onu
288       IF(ocdm .LT. 0.0_dp) THEN
289          PRINT*, "Error in compute_sigma: Omega_nu > Omega_m"
290          STOP
291       END IF
292
293       lower=log10(min)
294       upper=log10(max)
295       dkk = 0.0_dp
296       CALL gauleg(lower,upper,kk,dkk,n)
297
298       sum   = 0.0_dp
299       sumnu = 0.0_dp
300
301       DO i = 1,n
302          kki  = 10.0_dp**kk(i)
303          dkki = dkk(i)
304          CALL compute_pcdmlin(kki,om,h,power)
305          plin     = power
```

```
306         integ    = kki*kki*win8(kki)*win8(kki)*plin/(2._dp*PI_D*PI_D)
307         sum      = sum + integ * dkki * kki * log(10._dp)
308         plin_nu = power*powernu(kki,onu,h)
309         integnu = kki*kki*win8(kki)*win8(kki)*plin_nu/(2._dp*PI_D*PI_D)
310         sumnu    = sumnu + integnu * dkki * kki * log(10._dp)
311       END DO
312
313       norm     = s8*s8/sum
314       normnu   = s8*s8/sumnu
315
316     CONTAINS
317
318       FUNCTION win8(k)
319         ! A top-hat window function with R=8 Mpc/h.
320         IMPLICIT NONE
321
322         REAL(dp), INTENT(in) :: k
323         REAL(dp)             :: win8,kr
324
325         kr     = 8._dp * k
326
327         win8   = 3._dp*( SIN(kr)/(kr**3) - COS(kr)/(kr**2) )
328
329       END FUNCTION win8
330
331       FUNCTION powernu(k,onu,h)
332         IMPLICIT NONE
333
334         REAL(dp), INTENT(in) :: k,onu,h
335         REAL(dp)             :: powernu,Gamma,x,pot
336         REAL(dp), PARAMETER  :: e1 = 0.004321_dp
337         REAL(dp), PARAMETER  :: e2 = 2.217e-6_dp
338         REAL(dp), PARAMETER  :: e3 = 11.63_dp
339         REAL(dp), PARAMETER  :: e4 = 3.317_dp
340
341         Gamma = onu*h
342         x     = k/Gamma
343         pot   = onu**(1.05_dp)
344
345         powernu = ((1._dp+e1*x**(0.5_dp*e4)+e2*x**e4)/(1._dp+e3*x**e4))**pot
346
347       END FUNCTION powernu
348
349     END SUBROUTINE normalize_pdmlin
350
351   !!!!!!!!!!!!!!
352
353     SUBROUTINE compute_pcdmlin(k,om,h,power)
354
355       ! Computes the cold dark matter power spectrum, without
356       ! normalization constant.
```

```
357       IMPLICIT NONE
358
359       REAL(dp), INTENT(in) :: k,om,h
360       REAL(dp), INTENT(out):: power
361       REAL(dp)             :: Gamma,x,T,fac1,fac2
362       REAL(dp), PARAMETER  :: d1 = 2.34_dp
363       REAL(dp), PARAMETER  :: d2 = 3.89_dp
364       REAL(dp), PARAMETER  :: d3 = 16.1_dp
365       REAL(dp), PARAMETER  :: d4 = 5.46_dp
366       REAL(dp), PARAMETER  :: d5 = 6.71_dp
367
368       Gamma = om*h
369       x     = k/Gamma
370       fac1  = log(1._dp+d1*x)/(d1*x)
371       fac2  = 1._dp + d2*x + (d3*x)**2 +(d4*x)**3 + (d5*x)**4
372       T = fac1/(fac2**(0.25_dp))
373
374       power = k * T * T
375       RETURN
376     END SUBROUTINE compute_pcdmlin
377
378
379   !!!!!!!!!!!!!!!!!!!!!!!!!!!!!!!!!!!
380   !! READ PARAMETERS FROM TEXT FILE !!
381   !!!!!!!!!!!!!!!!!!!!!!!!!!!!!!!!!!!
382
383     SUBROUTINE read_params(filename,nk,nm,min_m,max_m,min_k,max_k)
384
385       IMPLICIT NONE
386       CHARACTER(LEN=128), INTENT(in)    :: filename
387       INTEGER(I4B),       INTENT(inout) :: nk,nm
388       REAL(DP),           INTENT(inout) :: min_m,max_m,min_k,max_k
389       CHARACTER(LEN=128) :: line, name, value
390       INTEGER(I4B)       :: rstat,i
391       LOGICAL(LGT)       :: exist
392       ! Checks if the file exists on disk. trim cuts the blank characters
393       ! away from filename
394       INQUIRE(file=filename, exist=exist)
395       IF(.NOT. exist) THEN
396          print *, "Error: File ", trim(filename) ," not found."
397          stop
398       END IF
399       PRINT '(/,"---------------------------------",/)'
400       PRINT*, "Your chosen parameters are"
401       PRINT*, " "
402       ! Reads the file line for line. Scan finds the index of the specified
403       ! character in the string. If there is no '=' on the line being read,
404       ! or there is a comment '#' on the line, the do loop skips to the next
405       ! line with cycle. Name contains the variable name, and value the value
406       ! of the variable. If the name corresponds to one of the cases, the
            value
```

```
407       ! of that name is inserted into the correct variable.
408       ! NOTE: If double precision values, write in 'd0' format.
409       open(unit=111, file=filename, form='formatted', iostat=rstat)
410       DO WHILE(rstat .EQ. 0)
411          read(unit=111, fmt='(A)',iostat=rstat) line
412          i = scan(line, '=')
413          IF ((i .EQ. 0) .OR.(line(1:1) .EQ. '#')) CYCLE
414          name = TRIM(adjustl(line(:i-1)))
415          value = TRIM(adjustl(line(i+1:)))
416
417          SELECT CASE(TRIM(name))
418          CASE('omega_nu')
419             read(value,*) omega_nu
420             print '(/,3x,"omega_nu = ",f10.2)',omega_nu
421          CASE('sigma8')
422             read(value,*) sigma8
423             print '(4x,"sigma8 = ",f10.2)',sigma8
424          CASE('nk')
425             read(value,*) nk
426             print '(/,8x,"nk = ",i10)',nk
427          CASE('nm')
428             read(value,*) nm
429             print '(8x,"nm = ",i10)',nm
430          CASE('min_m')
431             read(value,*) min_m
432             print '(5x,"min_m = ",es10.1)',min_m
433          CASE('max_m')
434             read(value,*) max_m
435             print '(5x,"max_m = ",es10.1)',max_m
436          CASE('min_k')
437             read(value,*) min_k
438             print '(5x,"min_k = ",es10.1)',min_k
439          CASE('max_k')
440             read(value,*) max_k
441             print '(5x,"max_k = ",es10.1)',max_k
442          END SELECT
443       END DO
444       PRINT '(/,"------------------------------",/)'
445       CLOSE(UNIT=111)
446
447    END SUBROUTINE read_params
448
449 END MODULE funcparams
450
451  !!!!!!!!!!!!!
452
453
454
455
456
457
```

```
!!!!!!!!!!!!!!!!!!!!!!!!!!!!!!!!!!!!!!!!!!!!!!!!!!!!!!
!! Here follows an example params.txt file:         !!
!!!!!!!!!!!!!!!!!!!!!!!!!!!!!!!!!!!!!!!!!!!!!!!!!!!!!!
!!                                                  !!
!! # cosmological parameters                        !!
!! omega_nu    = 0.05d0                             !!
!! sigma8      = 0.8d0                              !!
!! # loop variables in summing over mass and scale!!
!! nk          = 10000                              !!
!! nm          = 1000                               !!
!! min_m       = 1.0d6                              !!
!! max_m       = 1.0d20                             !!
!! min_k       = 0.01d0                             !!
!! max_k       = 1000.d0                            !!
!!                                                  !!
!!!!!!!!!!!!!!!!!!!!!!!!!!!!!!!!!!!!!!!!!!!!!!!!!!!!!!
```

Listing B.3: nrtype.f90

```
1  MODULE nrtype
2
3    ! symbolic names for kind types of 4-, 2- and 1-byte integers:
4    INTEGER, PARAMETER :: I4B = SELECTED_INT_KIND(9)
5    INTEGER, PARAMETER :: I2B = SELECTED_INT_KIND(4)
6    INTEGER, PARAMETER :: I1B = SELECTED_INT_KIND(2)
7
8    ! symbolic names for kind types of single- and double precision reals:
9    INTEGER, PARAMETER ::  SP = KIND(1.0)
10   INTEGER, PARAMETER ::  DP = KIND(1.0d0)
11
12   ! symbolic names for kind types of single, and double precision complex:
13   INTEGER, PARAMETER :: SPC = KIND((1.0,1.0))
14   INTEGER, PARAMETER :: DPC = KIND((1.0d0,1.0d0))
15
16   ! symbolic name for kind type of default logical:
17   INTEGER, PARAMETER :: LGT = KIND(.true.)
18
19   ! Frequently used mathematical constants (with precision to spare):
20   REAL(SP), PARAMETER :: pi     = 3.14159265358979323846264338327950288419
       _sp
21   REAL(SP), PARAMETER :: pio2   = 1.57079632679489661923132169163975144209858
       _sp
22   REAL(SP), PARAMETER :: twopi  = 6.28318530717958647692528676655900576839
       _sp
23   REAL(SP), PARAMETER :: sqrt2  = 1.41421356237309504880168872420969870856967
       _sp
24   REAL(SP), PARAMETER :: euler  = 0.57721566490153286060651209008240243104
       _sp
25   REAL(DP), PARAMETER :: pi_d   = 3.14159265358979323846264338327950288419
       _dp
26   REAL(DP), PARAMETER :: pio2_d = 1.57079632679489661923132169163975144209858
       _dp
27   REAL(SP), PARAMETER :: twopi_d= 6.28318530717958647692528676655900576839
       _dp
28   !self added:
29   REAL(DP), PARAMETER :: euler_d= 0.57721566490153286060651209008240243104
       _dp
30
31   ! The rest of this module is omitted, as it is not relevant.
32
33 END MODULE nrtype
```

Bibliography

[1] Barbara Ryden. *Introduction To Cosmology*. Pearson Education, Inc. Publishing as Addison Wesley, 2003.

[2] Scott Dodelson. *Modern Cosmology*. Academic Press/Elsevier, 2003.

[3] K. A. Olive and J. A. Peacock. Big Bang Cosmology. In *Yao, W.-M. et al.: Review of Particle Physics (online ed.)*. 2006. WEB address: http://pdg.lbl.org.

[4] Peter Schneider. *Extragalactic Astronomy and Cosmology: An Introduction*. Springer, 2006.

[5] Andrew R. Liddle and David H. Lyth. *Cosmological Inflation and Large-Scale Structure*. Cambridge University Press, 2000.

[6] Carlton Baugh. Correlation Function and Power Spectra in Cosmology. In P. Murdin, editor, *Encyclopedia of Astronomy and Astrophysics*. IoP Publishing Inc., 2006. WEB address: http://eaa.iop.org.

[7] A. Cooray and R. Sheth. Halo Models of Large Scale Structure. *Physics Reports*, 372:1, 2002.

[8] P. J. E. Peebles. *The Large-Scale Structure of the Universe*. Research supported by the National Science Foundation. Princeton, N.J., Princeton University Press. 435 p., 1980.

[9] M. Tegmark, M. Blanton, M. Strauss, F. Hoyle, D. Schlegel, R. Scoccimarro, M. Vogeley, D. Weinberg, I. Zehavi, A. Berlind, T. Budavari, A. Connolly, D. Eisenstein, D. Finkbeiner, J. Frieman, J. Gunn, A. Hamilton, L. Hui, B. Jain, D. Johnston, S. Kent, H. Lin, R. Nakajima, R. Nichol, J. Ostriker, A. Pope, R. Scranton, U. Seljak, R. Sheth, A. Stebbins, A. Szalay, I. Szapudi, L. Verde, Y. Xu, and 26 others for the SDSS Collaboration. The 3D power spectrum of galaxies from the SDSS. *ApJ*, 606:702, 2004.

[10] J. Dunkley, E. Komatsu, M. R. Nolta, D. N. Spergel, D. Larson, G. Hinshaw, L. Page, C. L. Bennett, B. Gold, N. Jarosik, J. L. Weiland, M. Halpern, R. S. Hill, A. Kogut, M. Limon, S. S. Meyer, G. S. Tucker, E. Wollack, and E. L. Wright. Five-Year

Wilkinson Microwave Anisotropy Probe (WMAP) Observations: Likelihoods and Parameters from the WMAP data. *ArXiv e-prints*, 803, March 2008. arXiv:0803.0586v1 [astro-ph].

[11] J. Neyman and E. L. Scott. A Theory of the Spatial Distribution of Galaxies. *ApJ*, 116:114, 1952.

[12] N. Kaizer. On the spatial correlations of Abell clusters. *ApJ*, 284:9, 1984.

[13] Julio F. Navarro, Carlos S. Frenk, and Simon D. M. White. The Structure of Cold Dark Matter Halos. *ApJ*, 462:563, 1996.

[14] L. Hernquist. An analytical model for spherical galaxies and bulges. *ApJ*, 356:359–364, June 1990.

[15] B. Moore, T. Quinn, F. Governato, J. Stadel, and G. Lake. Cold collapse and the core catastrophe. *MNRAS*, 310:1147–1152, December 1999.

[16] A. A. Collister and O. Lahav. Distribution of red and blue galaxies in groups: an empirical test of the halo model. *MNRAS*, 361:415–427, 2005.

[17] R. K. Sheth and G. Tormen. Large-scale bias and the peak background split. *MNRAS*, 308:119, 1999.

[18] Andrew R. Liddle, David H. Lyth, R. K. Schaefer, Q. Shafi, and Pedro T. P. Viana. Pursuing parameters for critical density dark matter models. *MNRAS*, 281:531, 1996.

[19] J. S Bullock, T. S. Kolatt, Y. Sigad, R. S. Somerville, A. V. Kravstov, A. A. Klypin, J. R. Primack, and A. Dekel. Profiles of dark haloes: evolution, scatter and environment. *MNRAS*, 321:559, 2001.

[20] W. H. Press, S. A. Teukolski, W. H. Vetterling, and B. P. Flannery. *Numerical Recipes in Fortran: The Art of Scientific Computing*. Cambridge University Press, 1992.

[21] J. M. Bardeen, J. R. Bond, N. Kaiser, and A. S. Szalay. The statistics of peaks of Gaussian random fields. *ApJ*, 304:15, 1986.

[22] C.-P. Ma. Linear Power Spectra in Cold+Hot Dark Matter Models: Analytical Approximations and Applications. *ApJ*, 471:13, 1996.

[23] W. H. Press, S. A. Teukolski, W. H. Vetterling, and B. P. Flannery. *Numerical Recipes in Fortran 90: The Art of Parallel Scientific Computing*. Cambridge University Press, 1996. Module `nrtype.f90` is available in the public domain at http://www.nr.com/pubdom/nrtype.f90.txt.

[24] R. K. Sheth, H. J. Mo, and G. Tormen. Ellipsoidal collapse and an improved model for the number and spatial distribution of dark matter halos. *MNRAS*, 323:1, 2001.

[25] WEB address: http://www.gnu.org/software/gsl/ (as of May 2008).